Title

Combined prokaryotic-eukaryotic delivery and expression of therapeutic factors through a primed autocatalytic positive-feedback loop

Author affiliation

Lei Shi [a], Bin Yu [a,b], Chun-Hui Cai [c,d], Wei Huang [e], Bo-Jian Zheng [f], David K. Smith [g], Jian-Dong Huang [a,h,*]

[a] *School of Biomedical Sciences and Shenzhen Institute of Research and Innovation, the University of Hong Kong, Pokfulam 999077, Hong Kong*

[b] *The Institute of Optoelectronics, Shenzhen University, Shenzhen 518060, PR China.*

[c] *Department of Obstetrics and Gynaecology, the University of Hong Kong, Pokfulam 999077, Hong Kong*

[d] *Advanced Institute of Translational Medicine, Tongji University School of Medicine, Shanghai 200092, PR China*

[e] *Faculty of Biology, South University of Science and Technology of China, Shenzhen 518055, PR China*

[f] *Department of Microbiology, the University of Hong Kong, Pokfulam 999077, Hong Kong.*

[g] *School of Public Health, the University of Hong Kong, Pokfulam 999077, Hong Kong*

[h] *The Centre for Synthetic Biology Engineering Research, Shenzhen Institutes of Advanced Technology, Shenzhen 518055, PR China.*

Corresponding author

* Correspondence and requests for materials should be addressed to Jian-Dong Huang.
Location: L3-72, Laboratory Block, the University of Hong Kong, 21 Sassoon Road, Hong Kong.
Office Phone: (852) 39172810
Email: jdhuang@hku.hk

Keywords:
Bacterial therapy
Tumor-targeting *Salmonella*
Inter-kingdom delivery and dual expression (IKDE)
Positive-feedback loop
Metastasis

Abstract

Progress in bacterial therapy for cancer and infectious diseases is hampered by the absence of safe and efficient vectors. Sustained delivery and high gene expression levels are critical for the therapeutic efficacy. Here we developed a *Salmonella typhimrium* strain to maintain and safely deliver a plasmid vector to target tissues. This vector is designed to allow dual transcription of therapeutic factors, such as cytotoxic proteins, short hairpin RNAs or combinations, in the nucleus or cytoplasm of eukaryotic cells, with this expression sustained by an autocatalytic positive-feedback loop. Mechanisms to prime the system and maintain the plasmid in the bacterium are also provided. Synergistic effects of attenuated *Salmonella* and our inter-kingdom system allow the precise expression of Diphtheria toxin A chain (DTA) gene in tumor microenvironment and eradicate large established tumors in immunocompetent animals. In the experiments reported here, 26% of mice (n=5/19) with aggressive tumors were cured and the other all survived until the end of the experiment. We also demonstrated that ST4 packaged with shRNA-encoding plasmids has sustained knockdown effects in nude mice bearing human MDA-MB-231 xenografts. Three weeks after injection of 5×10^6 ST4/pIKT-shPlk, *PLK1* transcript levels in tumors were 62.5 ± 18.6% lower than the vector control group (P=0.015). The presence of *PLK1* 5′ RACE-PCR cleavage products confirmed a sustained RNAi-mediated mechanism of action. This innovative technology provides an effective and versatile vehicle for efficient inter-kingdom gene delivery that can be applied to cancer therapy and other purposes.

1. Introduction

The use of bacteria as therapeutic agents has become an increasingly important area of investigation. Their low cost, fast production, diverse natural and modified tropism profiles, high packaging capacity, coupled with their relative tolerance of the immune system and relative ease of control in the case of adverse events, make bacterial-mediated delivery an attractive alternative for gastrointestinal [1], respiratory [2], urogenital tracts [3] and solid tumors [4, 5]. Most studies use attenuated bacteria in some way to decrease virulence [6-8] and augment their natural cytotoxicity with vectors designed to deliver an agent to the target organs [9-15]. However, to date, clinical trials of bacterial mediated therapy have had modest results [5, 16]. Limiting factors include the bacterial virulence [17], the effects of host immune response to their presence [18], the efficiency of intracellular delivery of multiple agents to target cells, instability of the plasmid vector leading to its loss in the bacteria [19], and inefficient transport of expression plasmids [20] to the nucleus to ensure an optimal dose level of therapeutic agents [21].

Using enhanced recombineering methods [22], we previously developed an "obligate" anaerobic *Salmonella* strain with enhanced host safety and anti-tumor activity [23, 24]. Here we build on that to develop a new platform that overcomes the above limitations while retaining some of its benefits. *S. typhimurium* strain SL7207, an *aroA* deficient strain [25] was used to engineer a series of *Salmonella* strains (Table S1) that have enhanced safety towards the host organism and an increased ability to deliver therapeutic payloads. We demonstrate a live microbe-based inter-kingdom system to deliver therapeutic vectors in a manner that does not compromise host safety and provides greatly improved stability, enhanced intracellular delivery and sustained expression of versatile therapeutic agents (including proteins or RNA molecules), which can target multiple gene networks.

Expression of the payloads is "primed" in mammalian cells through the transfer of both a therapeutic plasmid containing a foreign gene driven by dual promoters and an initial source of T7 RNA polymerase (T7 RNAP) enzyme, and propagated by an auto-feedback system. This therapeutic plasmid has been designed so that it can contain different payloads that are

capable of being expressed through both the cytoplasmic and nuclear systems in a mammalian cell and regulated by a feedback system. Maintenance of the plasmid in the bacterium is managed by relocating an essential bacterial gene *infA* from the bacterial chromosome onto the plasmid. It is the first report to date describing the design and use of a dual expression system incorporated with an amplification loop in gene therapy, which is based on an inter-kingdom interaction of bacteria and higher organisms. *In vivo* efficacy on tumor tissue and considerably improvement over existing techniques were demonstrated.

2. Materials and methods

2.1. Bacterial strains, animals, cell lines, enzymes and chemicals

Salmonella typhimurium strain SL7207 was kindly provided by Dr. B.A.D Stocker. Strains and plasmids are described in Table S1. Six-week-old female *nu*/*nu* athymic and BALB/c mice were purchased from the Laboratory Animal Unit of the University of Hong Kong. The research protocols were approved by the Committee on the Use of Live Animals in Teaching and Research of the University of Hong Kong (CULATR 1685-08). Breast cancer cell line MDA-MB-231 (human) and 4T1 (mouse) were from the American Type Culture Collection and cultured under conditions specified by the manufacturer. Enzymes were from New England Biolabs and chemicals were from Sigma-Aldrich

2.2. Construction of Salmonella mutants

The λ-Red recombination system (plasmid pSim6; a gift from Dr. Donald Court) was used to make genetic manipulations. A PCR-amplified *CM-T7 RNAP* cassette was electroporated into recombination-competent SL7207 cells and selected on chloramphenicol Luria-Bertani (LB) plates. The correct colony was confirmed by PCR and subsequently self-excised the antibiotic resistance, generating ST1. For the integration of Listeriolysin O （LLO）expression cassette, an integration vector backbone pYB-asd (a pBSK derivate with 1 kb flanking regions of *asd* sites) was generated. The *PsseA-hlyA* and *loxP-CM-loxP* cassettes were ligated to NotI, XhoI and XhoI respectively, to construct plasmid pYB-asd-hlyA. Then

the *CM-PsseA-hlyA* genetic circuit was digested by KpnI and SacII and transformed into ST1 cells induced for the λ-Red recombination to create strain ST2. Thirdly, a similar recombineering strategy was used to replace *htrA* gene by *CM-PpepT-asd-sodA* cassette in ST3. Fourthly, a 'precise' deletion of *infA* locus from ST3 has been performed. Plasmid pET28a-infA containing *E.coli* MG1655 *infA* expression cassette has been constructed and co-transformed with pSim6 into ST3. Strain ST5 was constructed similarly, but using *GFP* instead of *LLO*. A *tetR* selection cassette flanking with long homology arms of *infA* site was purified and transformed. PCR amplification of the new junctions between the drug marker and *infA* homology arm-flanking DNA was performed to confirm that the wild-type copy of *infA* was removed. The resulting strain ST4 was confirmed by colony PCR for site-specific integration of the targeting constructs (Table S2 and Fig. S1).

2.3. In vitro studies

Bacteria were harvested at the late logarithmic phase and then added at Multiplicity of infections (MOIs) ranging from 50 to 200 to cell monolayers. After 4 h, the cells were washed and grown for additional 24-72 h in complete medium containing 10 μg/ml of Gentamycin (Life Technologies).

Cells were arrested at G1 phase by double Thymidine block (at a concentration of 5 mM) or treated with 20 μg/ml Rifampicin, 1 μg/ml α-Amanitin or 1 μg/ml Cycloheximide to inhibit transcription or translation. To evaluate EGFP expression, total proteins were extracted by analysis buffer according to the GFP Quantization Kit (Biovision) and analysed by a Varioskan Flash spectral scanning multimode reader (Thermo Scientific). For quantification, the infected cells were detached and analysed by flow cytometry using a FACScalibur cytometer (Becton-Dickinson) and software WinMDI2.9.

Cell viability was measured using 5-diphenyltetrazolium bromide (MTT) according to the producer's protocol. For apoptosis assay, cells were harvested and stained with Annexin-V/ Propidium iodide (PI) assay kit (BD Biosciences), followed by flow cytometric analysis.

2.4. Tumor xenograft and in vivo studies

10^6 MDA-MB-231 cells or 10^5 4T1 cells were subcutaneously injected to athymic (*nu*/*nu*) or BALB/c mice. Tumor volume (mm^3) was determined by measuring length (l) and width (w) and calculating volumes ($V=lw^2/2$). Total RNA and protein were extracted from xenografted tumors following excision. The remaining tissues were divided in two longitudinally: one part was fixed in 4% paraformaldehyde (PFA) for subsequent hostological examinations, or to isolate ST4.

2.5. Real-time PCR quantification and western blot analysis

Total RNA was extracted by using TRIzol® (Life Technologies). Contaminating DNA was removed with DNase I and cDNA was generated using Superscript III First-strand Synthesis kit (Life Technologies). Anchored oligo $(dT)_{20}$ primer was used to hybridize to the poly (A) tail of mRNA transcribed from the nuclear system. Gene specific primers with an adapter were used to prime all the mRNA from both nuclear as well as cytoplasmic system. After cDNA synthesis, sequence-specific amplification was detected by a fluorescent signal of SYBR Green (ABI) by using Real-time PCR Detector (ABI7500). For western blotting, protein samples were separated on SDS-PAGE gels and then transferred to PVDF membranes (Millipore). Membranes were processed following the ECL western blotting protocol (Millipore).

2.6. ELISA assay of Diphtheria toxin A subunit

Briefly, 96-well plates were coated with a mouse anti-Diphtheria toxin A subunit (Maridian) monoclonal antibody in a dilution of 1:500 and blocked by PBS with 5% BSA. FLAG-tagged DT A chain was expressed by bacteria and purified by anti-FLAG M2 beads (Sigma-Aldrich). Protein concentration was determined by Bradford Reagent Assay. Tumor lysates were diluted in PBS with 2% BSA to concentrations within the liner range of the standard curve. A rabbit anti-FLAG antibody (Cell signalling) conjugated with horseradish peroxidase was used as the secondary antibody in a dilution of 1:8000.

2.7. Histology

Mice were intraperitoneally injected with a hypoxyprobe-1 solution (60 mg/kg) 10~40 min before euthanasia. Tissues were fixed in 4% PFA, paraffin embedded and sectioned into 5 μm slices. Hypoxic regions were visualized by mouse anti-hypoxyprobe-1 antibody (Chemicon), *Salmonella*, Diphtheria toxin A subunit, Plk1 and CD105 were separately detected by *Salmonella* (Abcam), Diphtheria toxin A subunit (Maridian), Plk1 (Life Technologies) or CD105 (PharMingen) antibody. Bound primary antibodies were detected using fluorescence conjugated secondary antibodies (Life Technologie) or HRP-conjugated secondary antibodies which then developed in DAB solution (Daco). Standard hematoxylin-eosin (H&E) staining was performed to detect histopathologic changes. The TUNEL working procedure was carried out following the producer's directions (Roche). Pictures were taken under a fluorescence microscope or a light microscope.

2.8. Culture of Salmonella ST4 from tissues

Tissues were homogenized in PBS (1:10 w/v ratio) and 10 μl of diluted (10^{-1}→10^{-5}) homogenate were dropped on LB agar plates supplemented with 0.5 mM DAP and 25 μg/ml streptomycin. These plates were incubated at 37 ℃ and examined for the presence of colonies.

2.9. 5'RACE assay for mRNA cleavage products

After first-strand cDNA synthesis, TdT (Terminal transferase) (Life Technologies) and dCTP (Life Technologies) was used to append a poly C^{+}-tail to the cDNA. Anchor primer UAP poly G and PLK1 GSP1 were used for the first around amplification of dC-tailed cDNA. Nested PCR was performed with 2 μl of the first reaction using the primer UAP and PLK1 GSP2. PCR products were examined by gel electrophoresis, and then cloned into T simple vector (Takara) for sequencing.

2.10. Isolation of murine serum

Murine blood was drawn into a serum vial and kept on ice. After congregation for 2 min at 16000×g, the supernatant serum was transferred in fresh tubes and stored -20℃ for further use. Serum alanine aminotransferase (ALT) and aspartate aminotransferase (AST) levels of mice were analysed by Reitman and Frankel method. Blood urea nitrogen (BUN) levels were determined by colorimetric method.

2.11. Statistics

Data are presented as mean ± standard deviation (SD). Statistical comparisons between two groups were evaluated by Student's t-test and corrected by ANOVA for multiple comparisons. Statistical significance was defined as P values of < 0.05. A log-rand test was used to compare xenograft survival. Prism 5.0 (GraphPad Software) provided the software for statistical analysis.

3. Results

3.1. Development of an Inter-kingdom Dual Expression System

S. typhimurium strain ST3 was engineered with multiple genetic modifications: (1) triple deletions of essential genes: *infA* for balanced-lethal host-vector system [26], and auxotrophic genes *aroA, asd* for further attenuation, (2) replacement of the *asd* gene with anaerobic control, (3) mutation of the colonic acid-producing gene *gmd* to preclude biofilm formation and enhance intracellular entry, (4) constitutive expression of T7 RNAP enzyme for priming transcription when the plasmid is delivered into the host cytoplasm, (5) intracellular expression of the pore-forming LLO (by replacing *asd* with *hlyA* gene from *Listeria monocytogenes*) to facilitate intracellular delivery of molecules to the host (Fig. S2). *In vitro* experiments demonstrated that ST3 could invade eukaryotic cells, break the endosomal compartment and directly release protein, plasmid DNA and translation-competent mRNA into the cytosol, leading to the desired gene expression (Fig. S3).

To develop a novel inter-kingdom dual expression (IKDE) system with a phage RNAP amplification circuit, a *T7 RNAP*-based cytoplasmic expression facility was added to the commonly used nuclear system. Transcription of the payloads is enabled by both T7 (cytoplasmic) and CMV (nuclear) promoters to allow a dual expression in the cytoplasm and nucleus respectively. Insertion of a eukaryotic internal ribosome entry site (IRES) prior to the gene of interest was added to augment RNA processing, allowing a cap-independent translation of transcripts produced in the mammalian cytoplasm [27] (Fig. 1A).

Initially *EGFP* was used as a foreign gene for a proof-of-concept experiment. Four plasmids harbouring an identical *EGFP* gene between an $IRES_{EMCV}$ element and a polyadenylation signal were constructed. *EGFP* gene was under the control of CMV promoter in pSD-EGFP, T7 promoter in pSR-EGFP, and a dual promoter in pSDR-EGFP. Plasmid pIKT-EGFP used both CMV and T7 promoters to control *EGFP* expression and had a *T7 RNAP* autogene cassette [28] (Fig. 1B). Kinetics of fluorescence expression in the cells following ST3-mediated delivery of an IKDE system versus the delivery of the other plasmids was evaluated (Fig. 1C). ST3/pIKT-EGFP produced the highest fluorescence intensity at all time points, with >10-fold increase in gene expression compared to plasmid DNA (pSD-EGFP) or DNA/RNA dual delivery (pSR-EGFP, pSDR-EGFP). Furthermore, we tested the effects of a series of inhibitors including prokaryotic mRNA transcription inhibitor (Rifampicin), eukaryotic transcription inhibitor (Amanitin), translation inhibitor (Cycloheximide) or cell cycle inhibitor (Thymidine) on reporter gene expression after infection and found that synthesis of EGFP observed by ST3/pIKT-EGFP infection with was mainly mediated by the direct eukaryotic translation of *EGFP* mRNA transcribed by the T7 RNAPs. Collectively, incorporation of T7 RNAP-based autocatalytic feedback loop enables a stable and continuous expression of *EGFP* assisted by self-amplification of the polymerases.

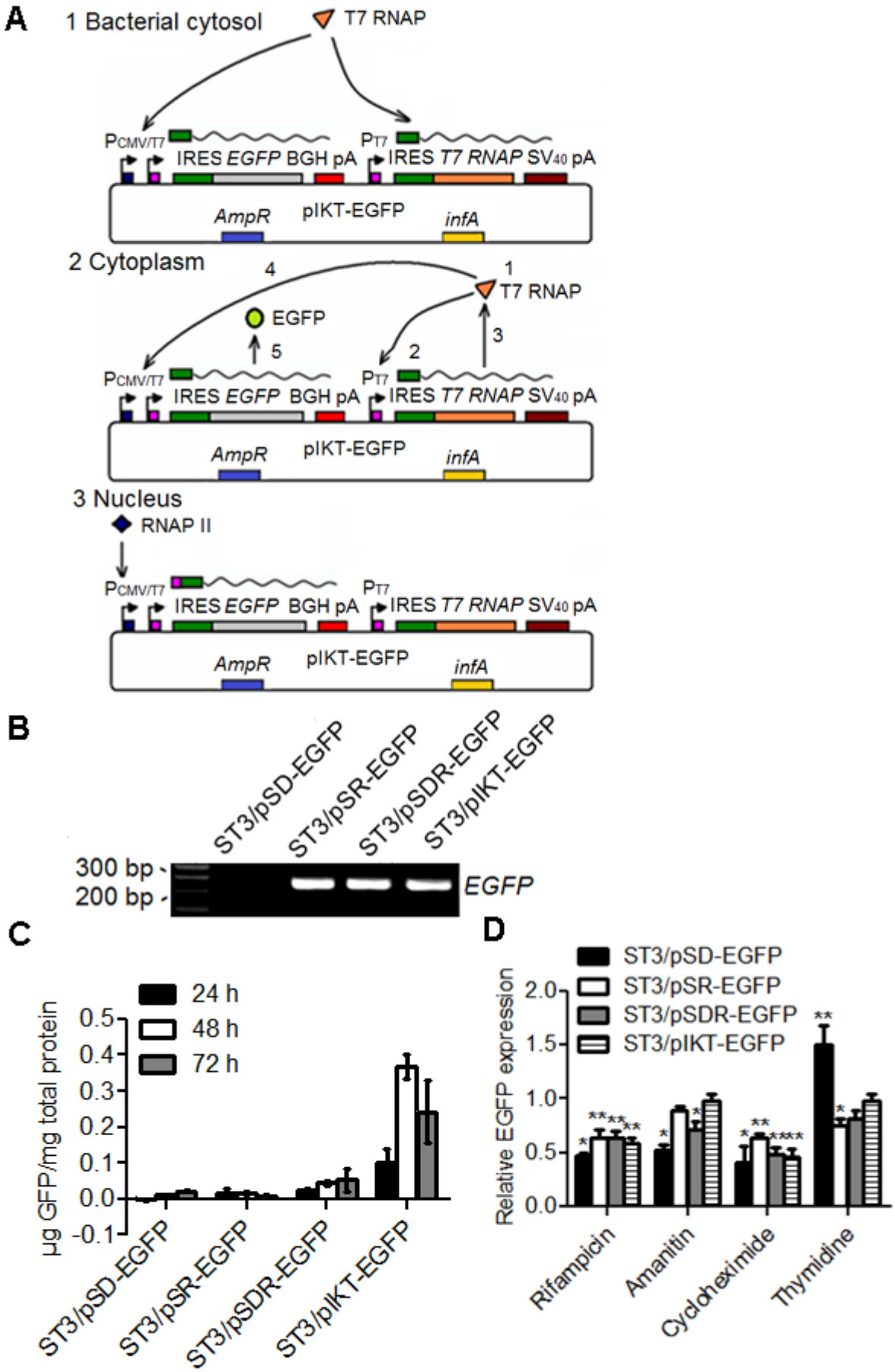
A
1 Bacterial cytosol
T7 RNAP
PCMV/T7
IRES EGFP BGH pA
PT7
IRES T7 RNAP SV40 pA
AmpR
pIKT-EGFP
infA
2 Cytoplasm
4
1
T7 RNAP
EGFP
5
2
3
3 Nucleus
RNAP II
B
ST3/pSD-EGFP
ST3/pSR-EGFP
ST3/pSDR-EGFP
ST3/pIKT-EGFP
300 bp
200 bp
EGFP
C
μg GFP/mg total protein
24 h
48 h
72 h
D
Relative EGFP expression
Rifampicin
Amanitin
Cycloheximide
Thymidine

Fig. 1. Delivery strain ST3 carrying an IKDE system leads to rapid and high-level transgene expression *in vitro.* (A) Schematic diagram of the IKDE system. (1) In the bacterial cytosol, bacterial chromosome-produced T7 RNAPs bind to the T7 promoter and then mediate the efficient transcription of mRNAs (curve). (2) Upon intracellular delivery, functional mRNAs will be translated into T7 RNAP (orange triangle) or EGFP (green circle) in the cytoplasm, where an initial source of T7 RNAPs can prime a positive-feedback loop and over-express gene mRNA from pIKT-EGFP (circle). (3) A small percentage of plasmid DNA will enter the nucleus, where the transcription machinery will generate stable transcripts through the nuclear system. (B) RT-PCR detection of *EGFP* mRNA in ST3 harbouring the indicated vectors. (C) Expression kinetics was determined at 24, 48 and 72 h post infections. Average GFP concentration and SD of three experiments are shown. (D) Fluorescent intensity of infected cells 40 h after infection in the presence of various inhibitors, relative to the level obtained in untreated controls. * $P<0.05$, ** $P<0.01$.

3.2. In vitro screening of potential therapeutic factors by ST3-mediated inter-kingdom gene transfer and RNAi

Using this synthetic inter-kingdom expression platform, intracellular delivery and expression of various cargos could be achieved to assess their therapeutic potential. ST3 harbouring different therapeutic candidates (Table S3), either protein, DNA or RNA, were used to deliver their cargos into MDA-MB-231 breast cancer cells.

When ST3 carrying a plasmid encoding therapeutic proteins, such as the catalytic fragment of diphtheria toxin (DTA), enters into the mammalian cells. Plasmids, T7 RNAP enzyme and translation-competent mRNA synthesized in the bacterium can pass into the cytoplasm, aided by the LLO generated pores, and then trigger the initial transcription of polymerases by the host (Fig. 2A). Driven by the T7 RNAP-autoactivation loop, gene expression substantially increases (Fig. 2B). Like therapeutic proteins, RNA therapeutic candidates, such as a shRNA against a cancer-related gene, can be delivered and transcribed from a similar plasmid, pIKT-shRNA, encoding a shRNA sequence under the control of T7 promoter. To evaluate the potency of ST3/pIKT-shRNA mediated knockdown of endogenous genes, a shRNA sequence shPlk, which targets a cell cycle-associated protein polo-like kinase 1 (PLK1) [29] was used (Fig. 2C). Quantitative real-time PCR was used to determine 6.89 ± 0.64 pg of shPlk present in 1 ng bacterial total RNA. By 48 h, ST3/pIKT-shPlk infection exhibited ~80% mRNA

inhibition and substantial protein reduction (Fig. 2D and E). A series of therapeutic factors were tested *in vitro* by measuring or monitoring physiological events such as cell death and proliferation (Fig. 2F). Lead candidates with relatively high potency were then evaluated in animal models.

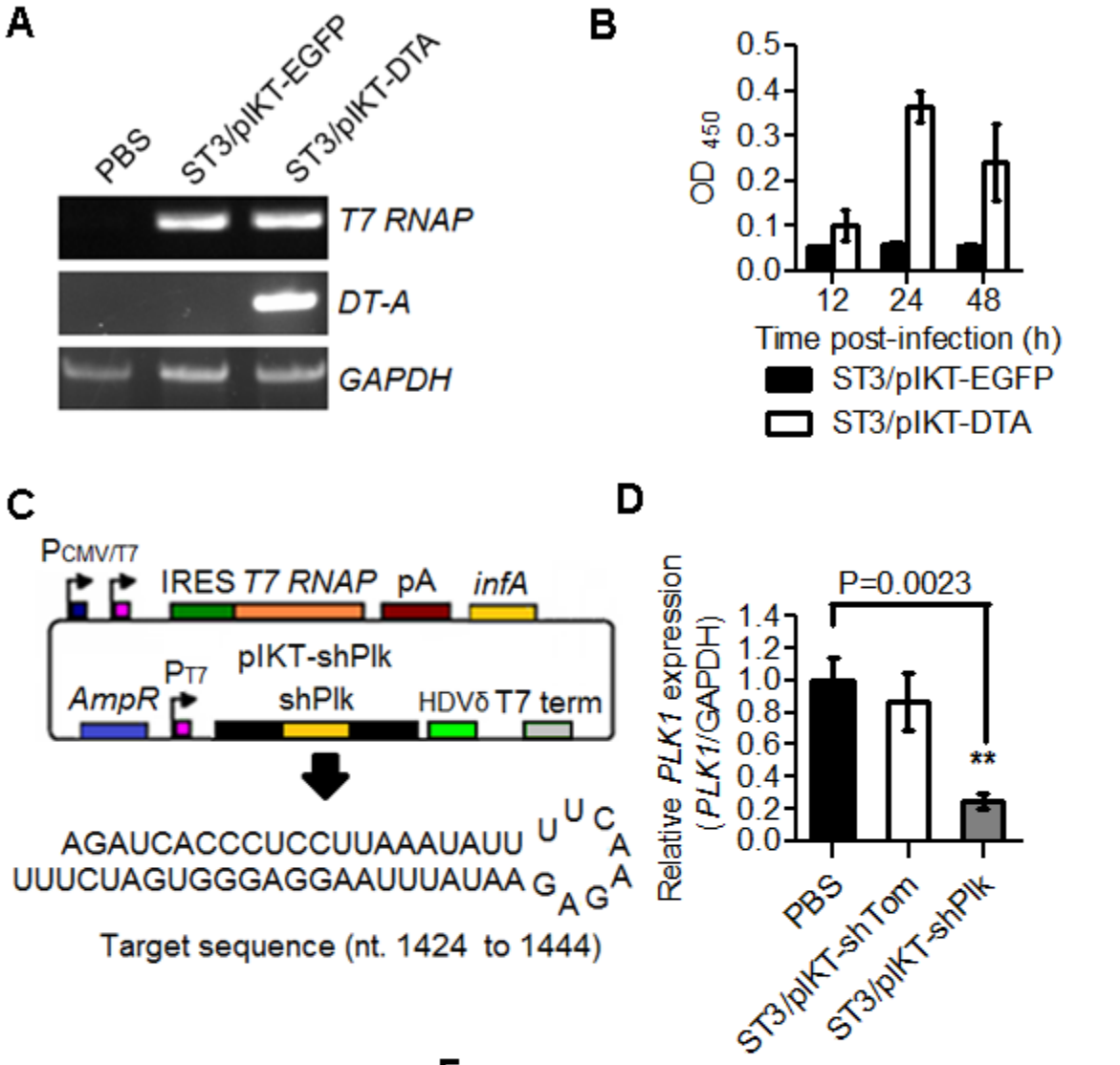
A
PBS
ST3/pIKT-EGFP
ST3/pIKT-DTA
T7 RNAP
DT-A
GAPDH
B
OD 450
0.5
0.4
0.3
0.2
0.1
0.0
12
24
48
Time post-infection (h)
ST3/pIKT-EGFP
ST3/pIKT-DTA
C
PCMV/T7
IRES T7 RNAP
pA
infA
pIKT-shPlk
PT7
AmpR
shPlk
HDVδ T7 term
AGAUCACCCUCCUUAAAUAUU
UUUCUAGUGGGAGGAAUUUAUAA
U U C A
G A G A
Target sequence (nt. 1424 to 1444)
D
Relative PLK1 expression (PLK1/GAPDH)
P=0.0023
**
1.4
1.2
1.0
0.8
0.6
0.4
0.2
0.0
PBS
ST3/pIKT-shTom
ST3/pIKT-shPlk
E
PBS
ST3/pIKT-shTom
ST3/pIKT-shPlk
Plk1
α-Tubulin
F
% Cell viability
% Apoptosis rate
120
100
80
60
40
20
0
PBS
EGFP
DTA
Endostatin
HA
PEA (II+III)
Shepherdin
sTRAIL
shTom
shCAT
shCCL18
shHer-2
shPlk
shTAK1
Let-7

Fig. 2. Inhibition of cell proliferation and induction of cell death by ST3-mediated inter-kingdom delivery and expression of a protein drug or hairpin RNA. (A) Human MDA-MB-231 cells were infected by ST3/pIKT-DTA or pIKT-EGFP. The cells were further cultured for 12 h before *T7 RNAP*, *DT-A* and *GAPDH* (control) transcripts were detected by RT-PCR. (B) The time course of DT-A expression was profiled for 48 h (n=3). (C) Plasmid diagram of pIKT-shPlk for transcription of shRNA against *PLK1*. (D) ~ 80% knockdown of target gene by ST3/pIKT-shPlk was verified by quantitative RT-PCR (n=4, **P<0.01). Data normalized to control values of 100%. (E) Western blot analysis confirmed the silencing effects on the protein levels. (F) Cell proliferation assay and Annexin-V/PI apoptosis analysis were assessed at 48 h post infections (n=3). All data are mean±SD.

3.3. ST4/pIKT-DTA therapy reduces tumor burden and malignant ascites while extending survival in the immunocompetent mice with highly aggressive tumors

Tumor-targeting *Salmonella* ST4 was modified from ST3 (Fig. S1), by placing the essential gene *asd* with a tightly hypoxic regulated control to program the bacterium only survive in anaerobic conditions (Fig. 3A), such as the hypoxic core of tumors (Fig. 3B). Injection of tumor-bearing nude mice with ST4 showed that the bacteria were replication-incompetent in normal organs but could amplify within tumors to as high as 10^8 cfu per gram tissue (Fig. 3C). Safety of strain ST4 was demonstrated in the immunocompromised animals, which could tolerate and survive for long periods, unlike the same hosts when infected with the parental bacterial strain (Fig. 3D and E).

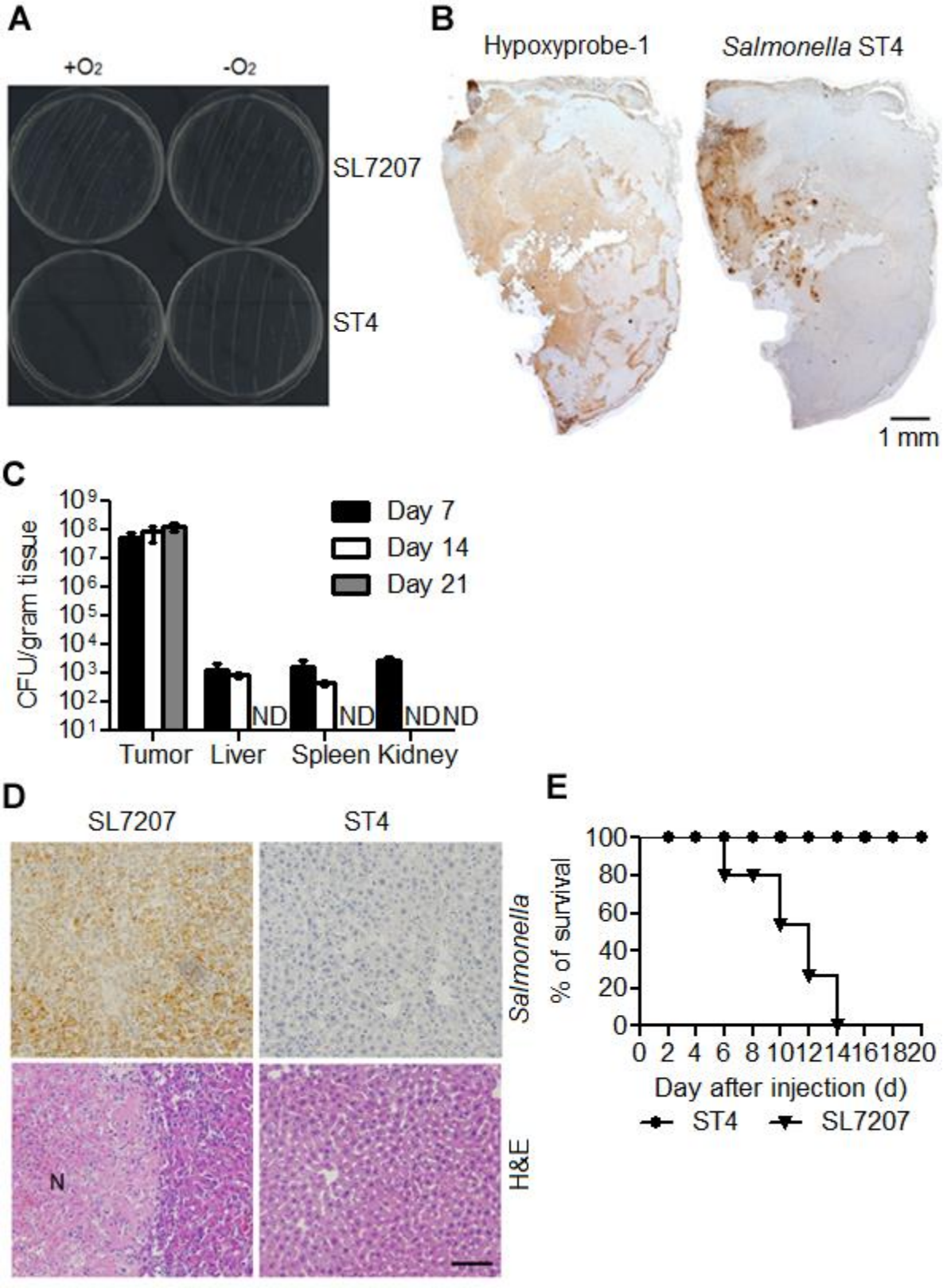
A
+O2
-O2
SL7207
ST4
B
Hypoxyprobe-1
Salmonella ST4
1 mm
C
CFU/gram tissue
Day 7
Day 14
Day 21
ND
ND
ND
ND
Tumor
Liver
Spleen
Kidney
D
SL7207
ST4
Salmonella
H&E
N
E
% of survival
Day after injection (d)
ST4
SL7207

Fig. 3. The conversion of wild-type strain SL7207 to ST4 could target the hypoxic core inside solid tumor and prevent the bacterial killing of the mice. (A) Strains SL7207 and ST4 were grown on LB agar plates under aerobic ($+O_2$) or anaerobic ($-O_2$) conditions. (B) Composite images were generated for the whole tumor to observe macroscopic bacterial colonization. A detailed examination of the distribution of ST4 inside the tumors revealed that the bacteria were resisted to the hypoxic regions (Hyperxyprobe-1 labelled). Scale bar, 1 mm. (C) Preferential accumulation of ST4 within the tumors after an intravenous injection (n=3). ND, not detected. (D) Lack of nonspecific accumulation of ST4 in the liver made improved safety. Representative histopathologic and immunohistochemical staining of *Salmonella* on liver sections as indicated. N, necrotic area. Scale bar, 100 μm. (E) Kaplan-Meier survival curves of the immunocompromised mice receiving ST4 or wild-type *Salmonella* at a dose of 5×10^7cells/mouse.

Next, we tested ST4 harbouring inter-kingdom dual expression of therapeutic proteins in an immunocompetent mouse model harbouring highly aggressive and metastatic breast cancer. 4T1 multidrug-resistant murine tumor cells were implanted into the mammary fat pad of immunocompetent, syngeneic BALB/c mice, which were subsequently inoculated with ST4/pIKT-DTA. After 7 and 14 days post-injection, bacteria were only growing in primary tumors and metastatic nodules in the lung and not found in normal tissues (Fig. 4A).

By day 2, production of *DT-A* was observed and its expression level was stably maintained over 2 weeks, after which the mice were sacrificed and primary tumors were harvested (Fig. 4B). Intracellular presence of bacterial toxins (red) in the cytosol of ST4/pIKT-DTA (green) infected cells, but not in ST4/pIKT-null infected counterparts was revealed by immunofluoresence and DAPI staining (Fig. 4C) and by western blot analysis (Fig. 4D). Immunohistochemical assay of tumor sections showed that polypeptides were diffused around the bacteria with some molecules transferred to the viable rim (Fig. S4). Total RNA was reverse transcribed using the target gene specific reverse anchor primer. Data showed that 92.7 ± 1.7% of the transcripts were driven by the T7 RNAP-based cytoplasmic expression, with the remainder driven by the nuclear specific CMV promoter.

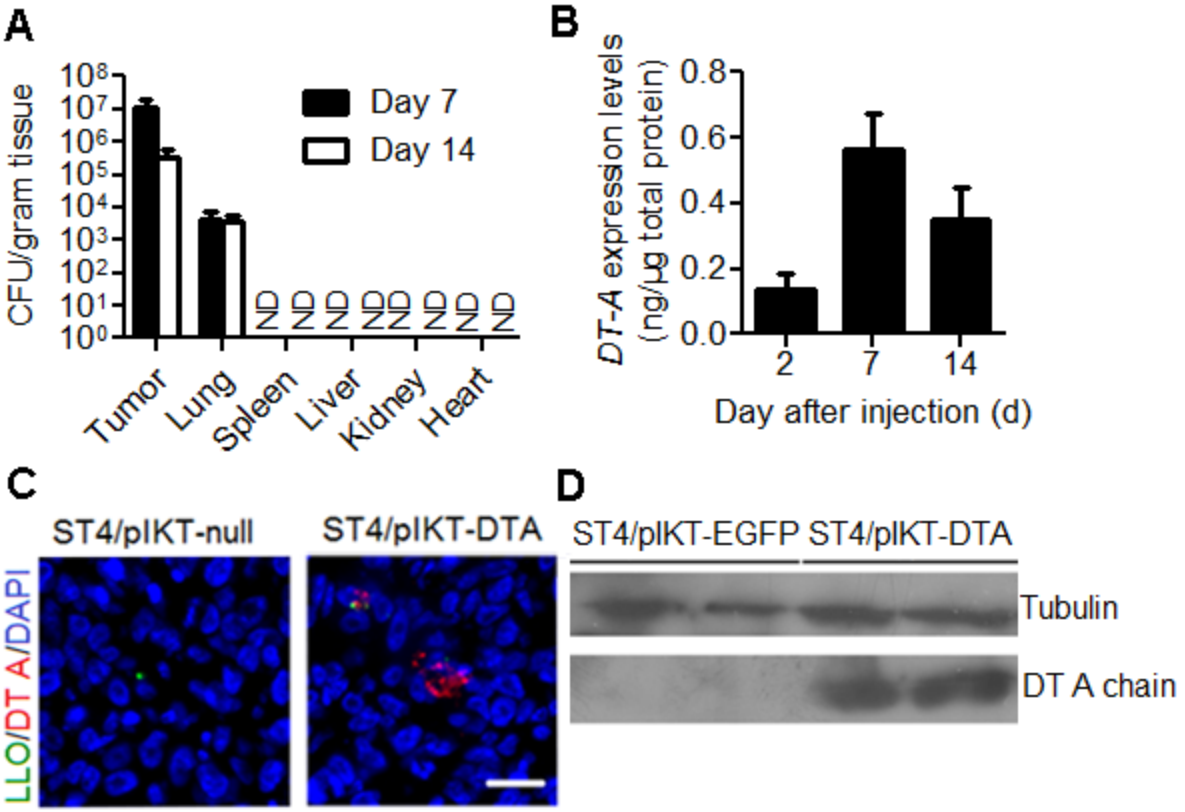

Fig. 4. Tumor-targeting *Salmonella* ST4 allows the precise expression of suicide gene in immunocompetent animals. (A) Bacterial accumulation in the tumors and normal tissues were determined 7 and 14 days later. Bars correspond to mean ± SD (n=3). ND, not detected. (B) Kinetics of *DT-A* expression over 2 weeks after a single ST4/pIKT-DTA injection. (C-D) Detection of suicide gene expression in the ST4/pIKT-DTA treated tumors by fluorescent immunostaining (C) and western blot analysis (D). (C) Tumor sections were stained for intracellular pore-forming LLO (green) and DT A chain (red). Scale bar, 25 μm.

In situ expression of DT A chain caused a much greater proportion of necrotic areas, significant cell death (1.8 ± 0.18 fold increase in TUNEL-positive cells) and an almost complete absence of proliferating Ki67-positive cells (Fig. 5A), compared to a control agent. Moreover, there were significant reductions in pulmonary metastases (P=0.025) in mouse models relative to ST4/pIKT-EGFP treatment (Fig. 5B), which had a slight inhibitory effect. Evidence to destruct tumor microenvironment by ST4/pIKT-DTA was also provided by CD105-immunohistochemical staining, indicating the destruction of blood vessels (Fig. S5).

Synergistic effects of attenuated *Salmonella* and the inter-kingdom system allowed the precise expression of DT A chain in tumor microenvironment and eradicated large established

tumors (Fig. S6). Another group consisted of animals carrying tumors of about 200~250 mm^3, which was found to be optimal for bacterial treatment. A single injection 5×10^6 of ST4/pIKT-DTA resulted in sustained regression over four weeks (Fig. 5C) and complete survival, whereas mice treated with PBS or ST4/pIKT-EGFP did not survive (Fig. 5D). Collectively, these experiments showed that ST4/pIKT-DTA treatment was effective in tumor shrinkage and greatly reduced the risk of death.

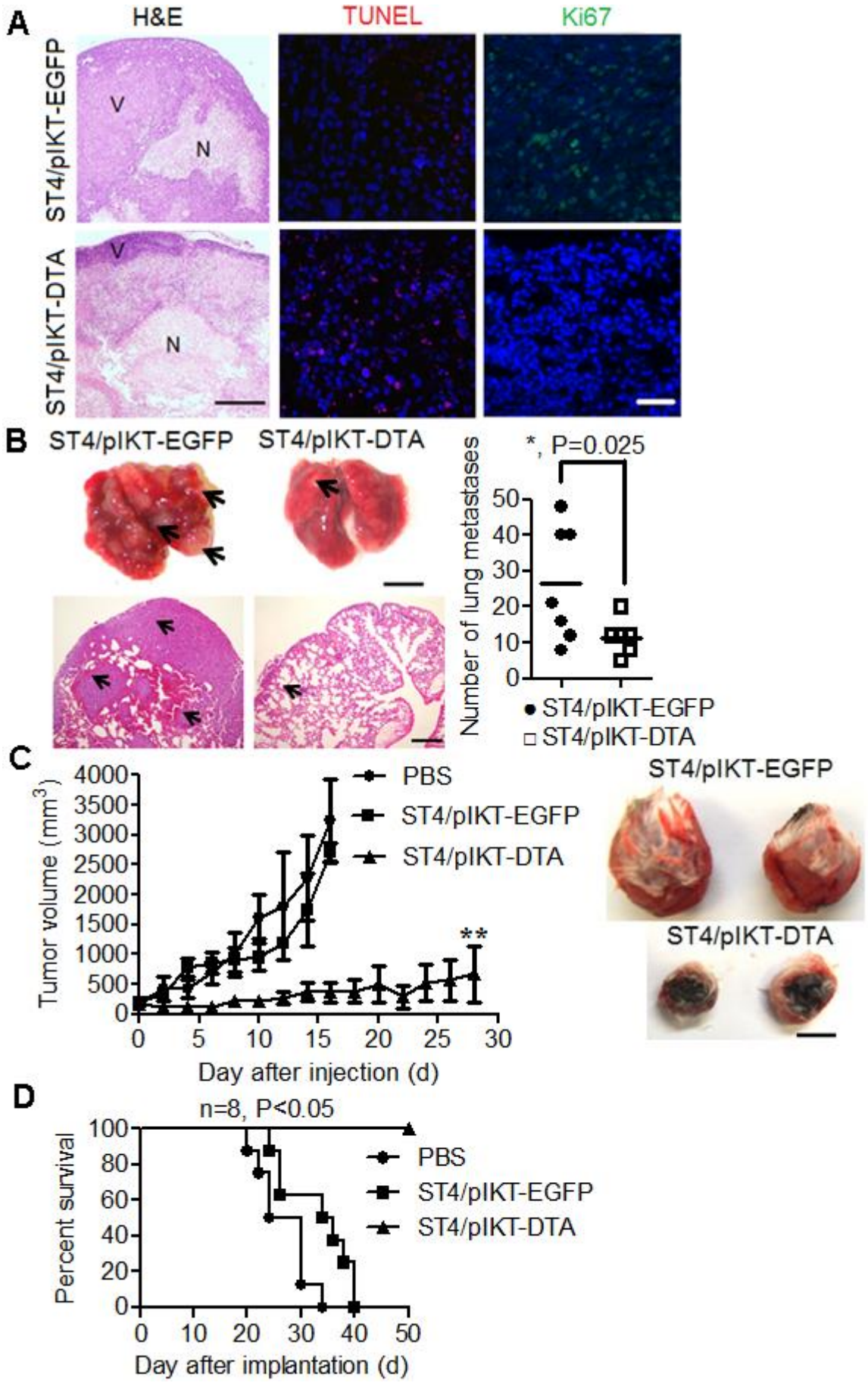
A
H&E
TUNEL
Ki67
ST4/pIKT-EGFP
ST4/pIKT-DTA
V
N
B
ST4/pIKT-EGFP
ST4/pIKT-DTA
*, P=0.025
Number of lung metastases
ST4/pIKT-EGFP
ST4/pIKT-DTA
C
Tumor volume (mm3)
PBS
ST4/pIKT-EGFP
ST4/pIKT-DTA
**
Day after injection (d)
ST4/pIKT-EGFP
ST4/pIKT-DTA
D
n=8, P<0.05
Percent survival
PBS
ST4/pIKT-EGFP
ST4/pIKT-DTA
Day after implantation (d)

Fig. 5. Potent therapeutic effects in immunocompetent mice with highly aggressive tumors elicited by ST4-mediated expression of diphtheria toxin. (A) Anti-tumor effects were examined by histological examination, apoptosis by TUNEL labelling and proliferation by Ki67 expression of primary tumors from ST4/pIKT-EGFP and ST4/pIKT-DTA treated mice. Viable regions are marked with V and the necrotic area by N. Scale bars, 500 μm for H&E staining; 50 μm for TUNEL and Ki67 staining. (B) Representative photographs of pulmonary metastases from mice treated as described above. Arrows indicate lung metastases. Scale bars, 1 cm for bright field imaging; 250 μm for H&E staining. Each dot represents the number of nodules per mouse. (C) On 12 day after tumor implantation, PBS, ST4/pIKT-EGFP or ST4/pIKT-DTA were intravenously injected to BALB/c mice with 4T1 breast tumors (n=5). Primary tumor volumes were measured every other day. (D) Kaplan-Meier survival curves of the animals administered with the indicated treatments (n=8), showing 100% survival only in the mice receiving ST4/pIKT-DTA treatment. All data are mean±SD. * P<0.05, ** P<0.01.

3.4. ST4-mediated inter-kingdom RNAi in vivo

We also demonstrated that ST4 packaged with shRNA-encoding plasmids has sustained knockdown effects in nude mice bearing human MDA-MB-231 xenografts. At three weeks after treatments, expression of *T7 RNAP* in the tumors, as confirmed by quantitative RT-PCR (159.1 ± 67.4 copies/ng RNA), was high and, as intended, led to enhanced shRNA production compared to inoculation with a system lacking this expression ability (ST4/pIKT△T7P-shPlk) (Fig. 6A). PLK1 transcript levels in tumors treated with ST4/pIKT-shPlk were 75.5 ± 11.5% (P=0.002) and 62.5 ± 18.6% (P=0.015) lower than those in mice injected with PBS (mock control) or ST4/pIKT-shTom (vector control) (Fig. 6B). The presence of *PLK1* 5′ RACE-PCR cleavage products confirmed a sustained RNAi-mediated mechanism of action (Fig. 6C, top). A clear reduction of PLK1 protein level was shown by western blot analysis (Fig. 6C, bottom) and immunohistochemical assay (Fig. 6D) only for ST4/pIKT-shPlk treated mice. No statistically significant induction of the interferon-inducible gene *OAS1* (encoding 2', 5'-oligoadenlylate synthetases) (P=0.16) was detected between ST4/pIKT-shTom and ST4/pIKT-shPlk treated mice, suggesting cytokine induction was not responsible for the observed knockdown effects. On day 20, tumor growth was restricted such that the tumor sizes in mice injected with PBS, ST4/pIKT-shTom and ST4/pIKT-shPlk were 2137.4 ± 170.2 mm^3, 1425.3± 136.0 mm^3 and 836.5 ± 166.7 mm^3, respectively, with ST4/pIKT-shPlk treated tumor sizes significantly smaller than those treated with ST4/pIKT-shTom (P<0.001) (Fig.

6E*)*. These results suggest that the ST4-mediated inter-kingdom RNAi induces a potent, specific and continuous gene silencing in solid tumors after a single injection.

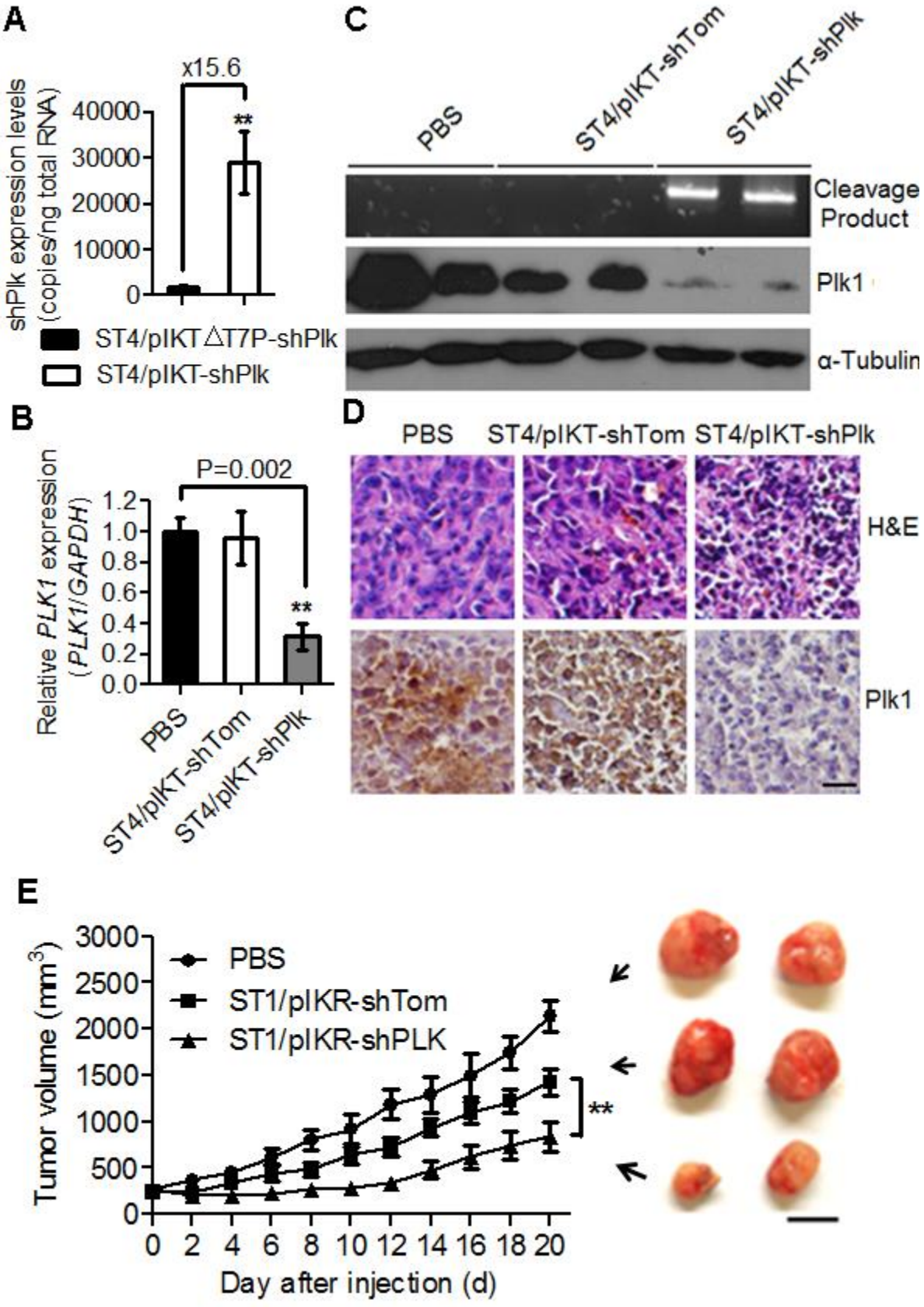

Fig. 6. Tumor-targeting ST4-mediated combinational inter-kingdom RNAi *in vivo*. (A) Quantitative stem-loop RT-PCR of shPlk1 levels in ST4/pIKT-shPlk and ST4/pIKRΔT7P-shPlk (without T7 RNAP autogene cassette) treated tumors (n=7). (B) Real-time PCR quantification of the reduction of *PLK1* mRNA after the indicated treatments (n=4). (C) Upper panel: *In vivo* 5'-RACE analysis of RNA extracted from ST4/pIKT-shPlk tumors confirmed the presence of specific cleaved product (414 bp). Lower panel: Western blot analysis of Plk1 and Tubulin protein levels in three groups. (D) Primary tumors were assessed by histological and immunohistochemical analyses. Sections stained with H&E (top) or probed with Plk1 antibody (bottom). Scale bar, 50 μm. (E) Tumor growth curves of mice (n=5 per group) treated with PBS, ST4/pIKT-shTom or ST4/pIKT-shPlk. All results are referred to mean±SD. ** $P<0.01$.

3.5. Systemic toxicity testing of ST4 harboring inter-kingdom therapeutic system to express cytotoxic proteins or shRNA

To evaluate the health status of mice during the bacterial treatments, the body weight and appearance of mice were monitored every other day. Body weight lost in the first 2~4 days and then recovered to the normal conditions during a 20-day observation period (Fig. 7A). All the mice have been sacrificed on day 20. Mice had slight enlarged spleens due to slight hematopoiesis (Fig. 7B). Serum ALT, AST and BUN levels in all treatment groups were in the normal range (Fig. 7C and D), which indicated no detectable hepatic stress or kidney injury. To investigate whether the bacterial infection or therapeutic molecules caused any pathological damages in the major organs, the sections of normal tissues have been processed for H&E staining (Fig. 7E). Gross morphological examination showed that there were no detectable abnormal nodules and apoptotic cell death in the selected organs. These indicated that systemic administration of one injection of ST4/pIKT-DTA or ST4/pIKT-shPlk was well tolerated at the dose level tested (5×10^6 cells/mouse) and the observed antitumor effects were unlikely related to toxic effects.

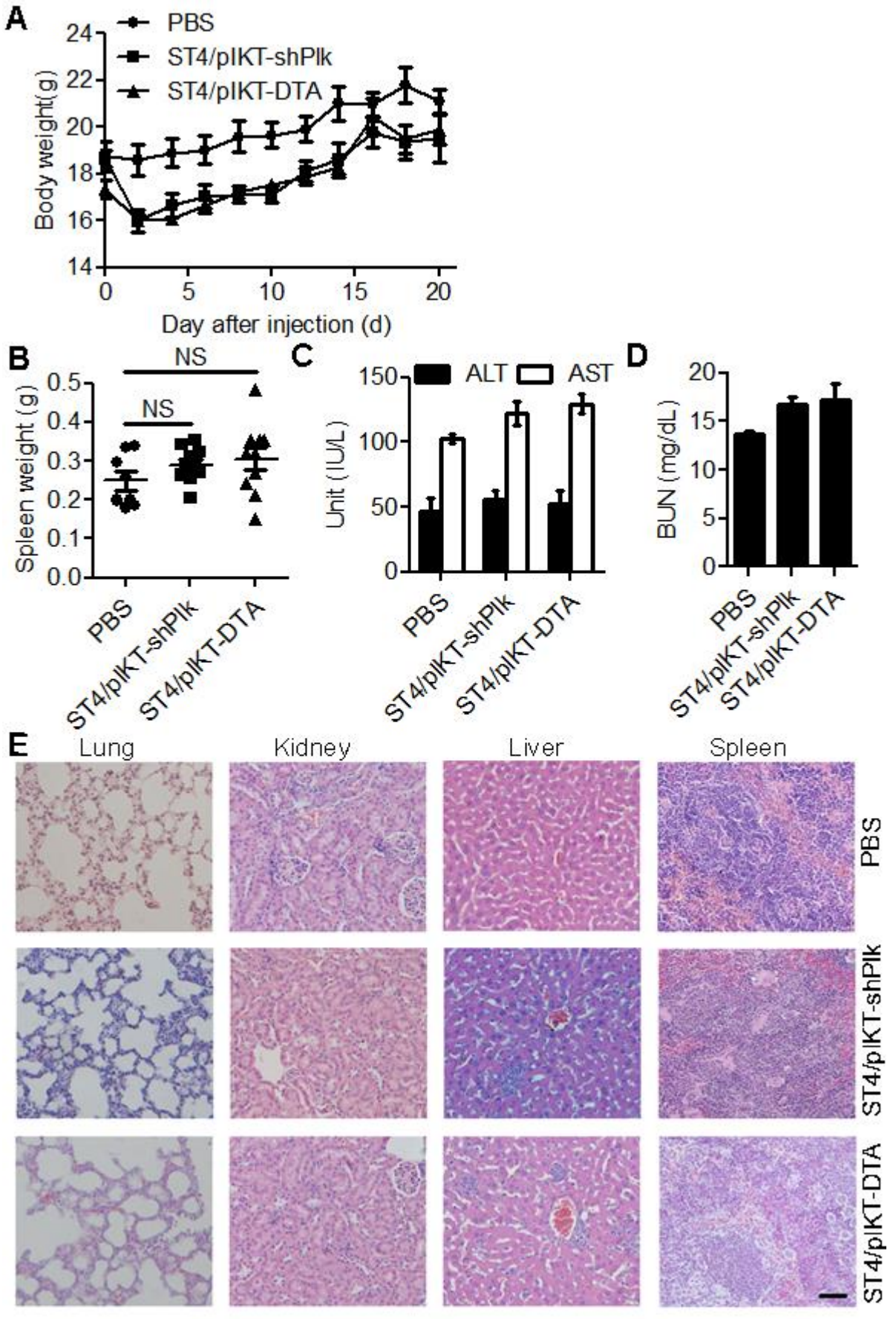
A
PBS
ST4/pIKT-shPlk
ST4/pIKT-DTA
Body weight(g)
Day after injection (d)
B
NS
NS
Spleen weight (g)
PBS
ST4/pIKT-shPlk
ST4/pIKT-DTA
C
ALT
AST
Unit (IU/L)
D
BUN (mg/dL)
E
Lung
Kidney
Liver
Spleen
PBS
ST4/pIKT-shPlk
ST4/pIKT-DTA

Fig. 7. Systemic toxicity testing of bacterial treatments. Body weight (A) and spleen weights (B) of tumor-bearing nude mice received with PBS, ST4/pIKT-shPlk or ST4/pIKT-DTA treatments. NS, no statistical significance. (C-D) Serum ALT, AST and BUN levels were measured by standard methods. Values are mean ± SD for 3 animals. (E) No apparent damage was found in any of the organs in either treatment group. Scale bar, 50 μm.

4. Discussion and conclusion

In the past decade, selected bacteria have been exploited as a tiny programmable robot factory and made great strides. Despite of a growing number of bacterial species that apparently exhibit intrinsic tumor-targeting properties, these bacteria generally been found to effective only against relatively small tumors in studies, and no bacterium that is able to inhibit tumor growth completely in fully immunocompetent hosts [30-36]. Our present study provides a considerable improvement over earlier technologies [13, 34, 37-39], in terms of safety, stability, flexibility and efficiency, and the following will highlight some reasons.

Some engineered *Salmonella* have exerted inherent tumor repression ability in many types of tumor models [33-36]. These attenuated *Salmonella* preferentially colonizes various human tumors; however, such bacteria would also colonize spleen and liver, achieving tumor-to-normal tissue accumulation ratios of 1000:1. This biodistribution may cause undesired side effects. To reduce intrinsic bacterial toxicity and achieve precise targeting of tumor microenvironment, a series of genetic manipulations based on the rational designed circuits has been made. After two or three weeks following injection, bacteria were barely detectable in normal organs (Fig. 3 C and D). These bacteria selectively grew within the primary tumors and also target to the metastases (Fig. 4A), which has been shown to be non-pathogenic in both immunocompetent and immunocompromised hosts (Fig. 3 D and E), suggesting that it is considered safe enough for therapeutic uses. In addition, our system is superior to previous bacterial systems in term of *in vivo* stability [12, 13]. Firstly, the bacterial factors involved in tumor fitness, intracellular delivery and expression were integrated into the chromosome. Secondly, we used a plasmid encoding a functional translation initiation factor1 from *E. coli* as selection marker and show that the expression vectors can be maintained in the *Salmonella* carriers at high copies *in vivo* (Table S4). This system is tightly

regulated due to no-cross feeding effects, which is superior to a selection system based on complementation of host auxotrophy [40].

The versatility of this inter-kingdom system was demonstrated by the use of a reporter gene as a proof of concept. Then the potent therapeutic results have been obtained through the synergistic antitumor effects of intrinsic bacterial toxicity plus the inter-kingdom expression of versatile therapeutic factors: bacterial toxins leading to cell death; and constructs for shRNA resulting in RNAi after processing in the target cells, as shown against the cell-cycle gene (*PLK1*). It was particularly notable that endowing these targeted bacteria to produce DT A chain greatly increase their antitumor activity in the immunocompetent animals, as determined in both subcutaneous primary tumor and lung metastases (Fig. 5). The likely reason for the improved inhibitory effect is that the killing-mediated by diphtheria toxin is direct and strong enough to eradicate multiple cell types, including the inflammatory cells and endothelial cells (Fig. S5), and subsequently destroy the tumor microenvironment. In the experiments reported here, a single dose of ST4/pIKT-DTA induced remarkable tumor shrinkage and cured 26% of cases (n=5/19).

Compared to the previously reported bacteria-mediated trans-kingdom RNAi [13], our technology has three improvements: (1) high tumor-targeting characteristics, (2) *in vivo* plasmid maintenance, (3) combination of prokaryotic and eukaryotic transcription of shRNA. *In vivo* studies suggested that ST4-mediated inter-kingdom RNAi system has achieved a stronger silencing ability and reduce total adverse effects (Fig. S7).

A series of pathological observations were also made to exclude non-specific toxicity of the above treatments being responsible for the observed effects (Fig. 7). Taken together, this combined bacterial and eukaryotic plasmid system may also have a place alongside established treatment and vaccination protocols.

Acknowledgments

This work was supported by a Collaborative Research Fund Grant from the Research Grants Council (RGC) of Hong Kong (HKU1/CRF/10), a National Basic Research Program

of China (973 Program, 2014CB745200) from the Ministry of Science and Technology of PRC, and a CRCG Seed Funding Program for Applied Research and to JDH, and a National Science Foundation of China (NSFC) grant No. 31200639 to BY. LS and JDH designed the experiment; LS, BY, CCH performed the experiments; LS, DKS and JDH wrote the manuscript. WH and BJZ provided essential reagents and critical comments. LS, BY and JDH have filed a regular application with the US Patent and Trademark Office on this work.

References

[1] J.L. Round, S.K. Mazmanian, The gut microbiota shapes intestinal immune responses during health and disease, Nat Rev Immunol, 9 (2009) 313-323.

[2] A.A. Bosch, G. Biesbroek, K. Trzcinski, E.A. Sanders, D. Bogaert, Viral and bacterial interactions in the upper respiratory tract, PLoS Pathog, 9 (2013) e1003057.

[3] R. Fujii, M. Iwahashi, K. Kikkawa, T. Inagaki, Y. Kohjimoto, T. Ojima, T. Mori, T. Kuramoto, S. Nishizawa, I. Azuma, H. Yamaue, T. Shinka, I. Hara, Bacillus Calmette-Guerin cell-wall skeleton enhances the killing activity of cytotoxic lymphocyte-activated human dendritic cells transduced with the prostate-specific antigen gene, BJU Int, 104 (2009) 1766-1773.

[4] C.H. Lee, Engineering bacteria toward tumor targeting for cancer treatment: current state and perspectives, Appl Microbiol Biot, 93 (2012) 517-523.

[5] N.S. Forbes, Engineering the perfect (bacterial) cancer therapy, Nat Rev Cancer, 10 (2010) 785-794.

[6] L.H. Dang, C. Bettegowda, D.L. Huso, K.W. Kinzler, B. Vogelstein, Combination bacteriolytic therapy for the treatment of experimental tumors, Proc Natl Acad Sci U S A, 98 (2001) 15155-15160.

[7] R.M. Hoffman, Tumor-seeking Salmonella amino acid auxotrophs, Curr Opin Biotechnol, 22 (2011) 917-923.

[8] V.H. Nguyen, H.S. Kim, J.M. Ha, Y.J. Hong, H.E. Choy, J.J. Min, Genetically Engineered Salmonella typhimurium as an Imageable Therapeutic Probe for Cancer, Cancer Res, 70 (2010) 18-23.

[9] H.Y. Zhang, J.H. Man, B. Liang, T. Zhou, C.H. Wang, T. Li, H.Y. Li, W.H. Li, B.F. Jin, P.J. Zhang, J. Zhao, X. Pan, K. He, W.L. Gong, X.M. Zhang, A.L. Li, Tumor-targeted delivery of biologically active TRAIL protein, Cancer Gene Ther, 17 (2010) 334-343.

[10] P. Wei, W.W. Wong, J.S. Park, E.E. Corcoran, S.G. Peisajovich, J.J. Onuffer, A. Weiss, W.A. Lim, Bacterial virulence proteins as tools to rewire kinase pathways in yeast and immune cells, Nature, 488 (2012) 384-388.

[11] R. Gardlik, M. Behuliak, R. Palffy, P. Celec, C.J. Li, Gene therapy for cancer: bacteria-mediated anti-angiogenesis therapy, Gene Ther, 18 (2011) 425-431.

[12] H. Guo, J. Zhang, C. Inal, T. Nguyen, J.H. Fruehauf, A.C. Keates, C.J. Li, Targeting tumor gene by shRNA-expressing Salmonella-mediated RNAi, Gene Ther, 18 (2011) 95-105.

[13] S. Xiang, J. Fruehauf, C.J. Li, Short hairpin RNA-expressing bacteria elicit RNA interference in mammals, Nat Biotechnol, 24 (2006) 697-702.

[14] S.N. Jiang, S.H. Park, H.J. Lee, J.H. Zheng, H.S. Kim, H.S. Bom, Y. Hong, M. Szardenings, M.G. Shin, S.C. Kim, V. Ntziachristos, H.E. Choy, J.J. Min, Engineering of bacteria for the visualization of targeted delivery of a cytolytic anticancer agent, Mol Ther, 21 (2013) 1985-1995.

[15] J.H. Jeong, K. Kim, D. Lim, K. Jeong, Y. Hong, V.H. Nguyen, T.H. Kim, S. Ryu, J.A. Lim, J.I. Kim, G.J. Kim, S.C. Kim, J.J. Min, H.E. Choy, Anti-tumoral effect of the mitochondrial target domain of Noxa delivered by an engineered Salmonella typhimurium, PLoS One, 9 (2014) e80050.

[16] N.J. Roberts, L. Zhang, F. Janku, A. Collins, R.Y. Bai, V. Staedtke, A.W. Rusk, D. Tung, M. Miller, J. Roix, K.V. Khanna, R. Murthy, R.S. Benjamin, T. Helgason, A.D. Szvalb, J.E. Bird, S. Roy-Chowdhuri, H.H. Zhang, Y. Qiao, B. Karim, J. McDaniel, A. Elpiner, A. Sahora, J. Lachowicz, B. Phillips, A. Turner, M.K. Klein, G. Post, L.A. Diaz, Jr., G.J. Riggins, N. Papadopoulos, K.W. Kinzler, B. Vogelstein, C. Bettegowda, D.L. Huso, M. Varterasian, S. Saha, S. Zhou, Intratumoral injection of Clostridium novyi-NT spores induces antitumor responses, Sci Transl Med, 6 (2014) 249ra111.
[17] Y. Zhang, N. Zhang, S. Su, R.M. Hoffman, M. Zhao, Salmonella typhimurium A1-R tumor targeting in immunocompetent mice is enhanced by a traditional Chinese medicine herbal mixture, Anticancer Res, 33 (2013) 1837-1843.
[18] K. Westphal, S. Leschner, J. Jablonska, H. Loessner, S. Weiss, Containment of tumor-colonizing bacteria by host neutrophils, Cancer Res, 68 (2008) 2952-2960.
[19] S.Y. Zheng, B. Yu, K. Zhang, M. Chen, Y.H. Hua, S. Yuan, R.M. Watt, B.J. Zheng, K.Y. Yuen, J.D. Huang, Comparative immunological evaluation of recombinant Salmonella Typhimurium strains expressing model antigens as live oral vaccines, BMC Immunol, 13 (2012) 54.
[20] A. Zelmer, S. Krusch, A. Koschinski, M. Rohde, H. Repp, T. Chakraborty, S. Weiss, Functional transfer of eukaryotic expression plasmids to mammalian cells by Listeria monocytogenes: a mechanistic approach, J Gene Med, 7 (2005) 1097-1112.
[21] M.D. Larsen, U. Griesenbach, S. Goussard, D.C. Gruenert, D.M. Geddes, R.K. Scheule, S.H. Cheng, P. Courvalin, C. Grillot-Courvalin, E.W. Alton, Bactofection of lung epithelial cells in vitro and in vivo using a genetically modified Escherichia coli, Gene Ther, 15 (2008) 434-442.
[22] B. Yu, M. Yang, H.Y.B. Wong, R.M. Watt, E.W. Song, B.J. Zheng, K.Y. Yuen, J.D. Huang, A method to generate recombinant Salmonella typhi Ty21a strains expressing multiple heterologous genes using an improved recombineering strategy, Appl Microbiol Biot, 91 (2011) 177-188.
[23] B. Yu, M. Yang, L. Shi, Y. Yao, Q. Jiang, X. Li, L.H. Tang, B.J. Zheng, K.Y. Yuen, D.K. Smith, E. Song, J.D. Huang, Explicit hypoxia targeting with tumor suppression by creating an "obligate" anaerobic Salmonella Typhimurium strain, Sci Rep, 2 (2012) 436.
[24] Z.L. Guo, B. Yu, B.T. Ning, S. Chan, Q.B. Lin, J.C. Li, J.D. Huang, G.C. Chan, Genetically modified "obligate" anaerobic Salmonella typhimurium as a therapeutic strategy for neuroblastoma, J Hematol Oncol, 8 (2015) 99.
[25] S.K. Hoiseth, B.A. Stocker, Aromatic-dependent Salmonella typhimurium are non-virulent and effective as live vaccines, Nature, 291 (1981) 238-239.
[26] P. Hagg, J.W. de Pohl, F. Abdulkarim, L.A. Isaksson, A host/plasmid system that is not dependent on antibiotics and antibiotic resistance genes for stable plasmid maintenance in Escherichia coli, J Biotechnol, 111 (2004) 17-30.
[27] J. Finn, A.C. Lee, I. MacLachlan, P. Cullis, An enhanced autogene-based dual-promoter cytoplasmic expression system yields increased gene expression, Gene Ther, 11 (2004) 276-283.

[28] M. Brisson, Y. He, S. Li, J.P. Yang, L. Huang, A novel T7 RNA polymerase autogene for efficient cytoplasmic expression of target genes, Gene Ther, 6 (1999) 263-270.
[29] X. Liu, M. Lei, R.L. Erikson, Normal cells, but not cancer cells, survive severe Plk1 depletion, Mol Cell Biol, 26 (2006) 2093-2108.
[30] S. Ganai, R.B. Arenas, N.S. Forbes, Tumour-targeted delivery of TRAIL using Salmonella typhimurium enhances breast cancer survival in mice, Br J Cancer, 101 (2009) 1683-1691.
[31] N. Agrawal, C. Bettegowda, I. Cheong, J.F. Geschwind, C.G. Drake, E.L. Hipkiss, M. Tatsumi, L.H. Dang, L.A. Diaz, M. Pomper, M. Abusedera, R.L. Wahl, K.W. Kinzler, S.B. Zhou, D.L. Huso, B. Vogelstein, Bacteriolytic therapy can generate a potent immune response against experimental tumors, Proc Natl Acad Sci U S A, 101 (2004) 15172-15177.
[32] W. Quispe-Tintaya, D. Chandra, A. Jahangir, M. Harris, A. Casadevall, E. Dadachova, C. Gravekamp, Nontoxic radioactive Listeria(at) is a highly effective therapy against metastatic pancreatic cancer, Proc Natl Acad Sci U S A, 110 (2013) 8668-8673.
[33] Y. Matsumoto, S. Miwa, Y. Zhang, M. Zhao, S. Yano, F. Uehara, M. Yamamoto, Y. Hiroshima, M. Toneri, M. Bouvet, H. Matsubara, H. Tsuchiya, R.M. Hoffman, Intraperitoneal administration of tumor-targeting Salmonella typhimurium A1-R inhibits disseminated human ovarian cancer and extends survival in nude mice, Oncotarget, 6 (2015) 11369-11377.
[34] M. Zhao, J. Geller, H. Ma, M. Yang, S. Penman, R.M. Hoffman, Monotherapy with a tumor-targeting mutant of Salmonella typhimurium cures orthotopic metastatic mouse models of human prostate cancer, Proc Natl Acad Sci U S A, 104 (2007) 10170-10174.
[35] Y. Hiroshima, M. Zhao, Y. Zhang, A. Maawy, M.K. Hassanein, F. Uehara, S. Miwa, S. Yano, M. Momiyama, A. Suetsugu, T. Chishima, K. Tanaka, M. Bouvet, I. Endo, R.M. Hoffman, Comparison of efficacy of Salmonella typhimurium A1-R and chemotherapy on stem-like and non-stem human pancreatic cancer cells, Cell Cycle, 12 (2013) 2774-2780.
[36] Y. Matsumoto, S. Miwa, Y. Zhang, Y. Hiroshima, S. Yano, F. Uehara, M. Yamamoto, M. Toneri, M. Bouvet, H. Matsubara, R.M. Hoffman, M. Zhao, Efficacy of tumor-targeting Salmonella typhimurium A1-R on nude mouse models of metastatic and disseminated human ovarian cancer, J Cell Biochem, 115 (2014) 1996-2003.
[37] R. Palffy, R. Gardlik, J. Hodosy, M. Behuliak, P. Resko, J. Radvansky, P. Celec, Bacteria in gene therapy: bactofection versus alternative gene therapy, Gene Ther, 13 (2006) 101-105.
[38] H. Bauer, A. Darji, T. Chakraborty, S. Weiss, Salmonella-mediated oral DNA vaccination using stabilized eukaryotic expression plasmids, Gene Ther, 12 (2005) 364-372.
[39] S. Xiang, A.C. Keates, J. Fruehauf, Y. Yang, H. Guo, T. Nguyen, C.J. Li, In vitro and in vivo gene silencing by TransKingdom RNAi (tkRNAi), Methods Mol Biol, 487 (2009) 147-160.
[40] J.J. Min, V.H. Nguyen, H.J. Kim, Y. Hong, H.E. Choy, Quantitative bioluminescence imaging of tumor-targeting bacteria in living animals, Nat Protoc, 3 (2008) 629-636.

Figure legends

Fig. 1. Delivery strain ST3 carrying an IKDE system leads to rapid and high-level transgene expression *in vitro.* (A) Schematic diagram of the IKDE system. (1) In the bacterial cytosol, bacterial chromosome-produced T7 RNAPs bind to the T7 promoter and then mediate the efficient transcription of mRNAs (curve). (2) Upon intracellular delivery, functional mRNAs will be translated into T7 RNAP (orange triangle) or EGFP (green circle) in the cytoplasm, where an initial source of T7 RNAPs can prime a positive-feedback loop and over-express gene mRNA from pIKT-EGFP (circle). (3) A small percentage of plasmid DNA will enter the nucleus, where the transcription machinery will generate stable transcripts through the nuclear system. (B) RT-PCR detection of *EGFP* mRNA in ST3 harbouring the indicated vectors. (C) Expression kinetics was determined at 24, 48 and 72 h post infections. Average GFP concentration and SD of three experiments are shown. (D) Fluorescent intensity of infected cells 40 h after infection in the presence of various inhibitors, relative to the level obtained in untreated controls. * $P<0.05$, ** $P<0.01$.

Fig. 2. Inhibition of cell proliferation and induction of cell death by ST3-mediated inter-kingdom delivery and expression of a protein drug or hairpin RNA. (A) Human MDA-MB-231 cells were infected by ST3/pIKT-DTA or pIKT-EGFP. The cells were further cultured for 12 h before *T7 RNAP, DT-A* and *GAPDH* (control) transcripts were detected by RT-PCR. (B) The time course of DT-A expression was profiled for 48 h (n=3). (C) Plasmid diagram of pIKT-shPlk for transcription of shRNA against *PLK1*. (D) ~ 80% knockdown of target gene by ST3/pIKT-shPlk was verified by quantitative RT-PCR (n=4, **$P<0.01$). Data normalized to control values of 100%. (E) Western blot analysis confirmed the silencing effects on the protein levels. (F) Cell proliferation assay and Annexin-V/PI apoptosis analysis were assessed at 48 h post infections (n=3). All data are mean$\pm$SD.

Fig. 3. The conversion of wild-type strain SL7207 to ST4 could target the hypoxic core inside solid tumor and prevent the bacterial killing of the mice. (A) Strains SL7207 and ST4 were grown on LB agar plates under aerobic ($+O_2$) or anaerobic ($-O_2$) conditions. (B) Composite images were generated for the whole tumor to observe macroscopic bacterial colonization. A detailed examination of the distribution of ST4 inside the tumors revealed that the bacteria were resisted to the hypoxic regions (Hyperxyprobe-1 labelled). Scale bar, 1 mm. (C) Preferential accumulation of ST4 within the tumors after an intravenous injection (n=3). ND, not detected. (D) Lack of nonspecific accumulation of ST4 in the liver made improved safety. Representative histopathologic and immunohistochemical staining of *Salmonella* on liver sections as indicated. N, necrotic area. Scale bar, 100 μm. (E) Kaplan-Meier survival curves of the immunocompromised mice receiving ST4 or wild-type *Salmonella* at a dose of 5×10^7cells/mouse.

Fig. 4. Tumor-targeting *Salmonella* ST4 allows the precise expression of suicide gene in immunocompetent animals. (A) Bacterial accumulation in the tumors and normal tissues were

determined 7 and 14 days later. Bars correspond to mean ± SD (n=3). ND, not detected. (B) Kinetics of *DT-A* expression over 2 weeks after a single ST4/pIKT-DTA injection. (C-D) Detection of suicide gene expression in the ST4/pIKT-DTA treated tumors by fluorescent immunostaining (C) and western blot analysis (D). (C) Tumor sections were stained for intracellular pore-forming LLO (green) and DT A chain (red). Scale bar, 25 μm.

Fig. 5. Potent therapeutic effects in immunocompetent mice with highly aggressive tumors elicited by ST4-mediated expression of diphtheria toxin. (A) Anti-tumor effects were examined by histological examination, apoptosis by TUNEL labelling and proliferation by Ki67 expression of primary tumors from ST4/pIKT-EGFP and ST4/pIKT-DTA treated mice. Viable regions are marked with V and the necrotic area by N. Scale bars, 500 μm for H&E staining; 50 μm for TUNEL and Ki67 staining. (B) Representative photographs of pulmonary metastases from mice treated as described above. Arrows indicate lung metastases. Scale bars, 1 cm for bright field imaging; 250 μm for H&E staining. Each dot represents the number of nodules per mouse. (C) On 12 day after tumor implantation, PBS, ST4/pIKT-EGFP or ST4/pIKT-DTA were intravenously injected to BALB/c mice with 4T1 breast tumors (n=5). Primary tumor volumes were measured every other day. (D) Kaplan-Meier survival curves of the animals administered with the indicated treatments (n=8), showing 100% survival only in the mice receiving ST4/pIKT-DTA treatment. All data are mean±SD. * $P<0.05$, ** $P<0.01$.

Fig. 6. Tumor-targeting ST4-mediated combinational inter-kingdom RNAi *in vivo*. (A) Quantitative stem-loop RT-PCR of shPlk1 levels in ST4/pIKT-shPlk and ST4/pIKRΔT7P-shPlk (without T7 RNAP autogene cassette) treated tumors (n=7). (B) Real-time PCR quantification of the reduction of *PLK1* mRNA after the indicated treatments (n=4). (C) Upper panel: *In vivo* 5'-RACE analysis of RNA extracted from ST4/pIKT-shPlk tumors confirmed the presence of specific cleaved product (414 bp). Lower panel: Western blot analysis of Plk1 and Tubulin protein levels in three groups. (D) Primary tumors were assessed by histological and immunohistochemical analyses. Sections stained with H&E (top) or probed with Plk1 antibody (bottom). Scale bar, 50 μm. (E) Tumor growth curves of mice (n=5 per group) treated with PBS, ST4/pIKT-shTom or ST4/pIKT-shPlk. All results are referred to mean±SD. ** $P<0.01$.

Fig. 7. Systemic toxicity testing of bacterial treatments. Body weight (A) and spleen weights (B) of tumor-bearing nude mice received with PBS, ST4/pIKT-shPlk or ST4/pIKT-DTA treatments. NS, no statistical significance. (C-D) Serum ALT, AST and BUN levels were measured by standard methods. Values are mean ± SD for 3 animals. (E) No apparent damage was found in any of the organs in either treatment group. Scale bar, 50 μm.

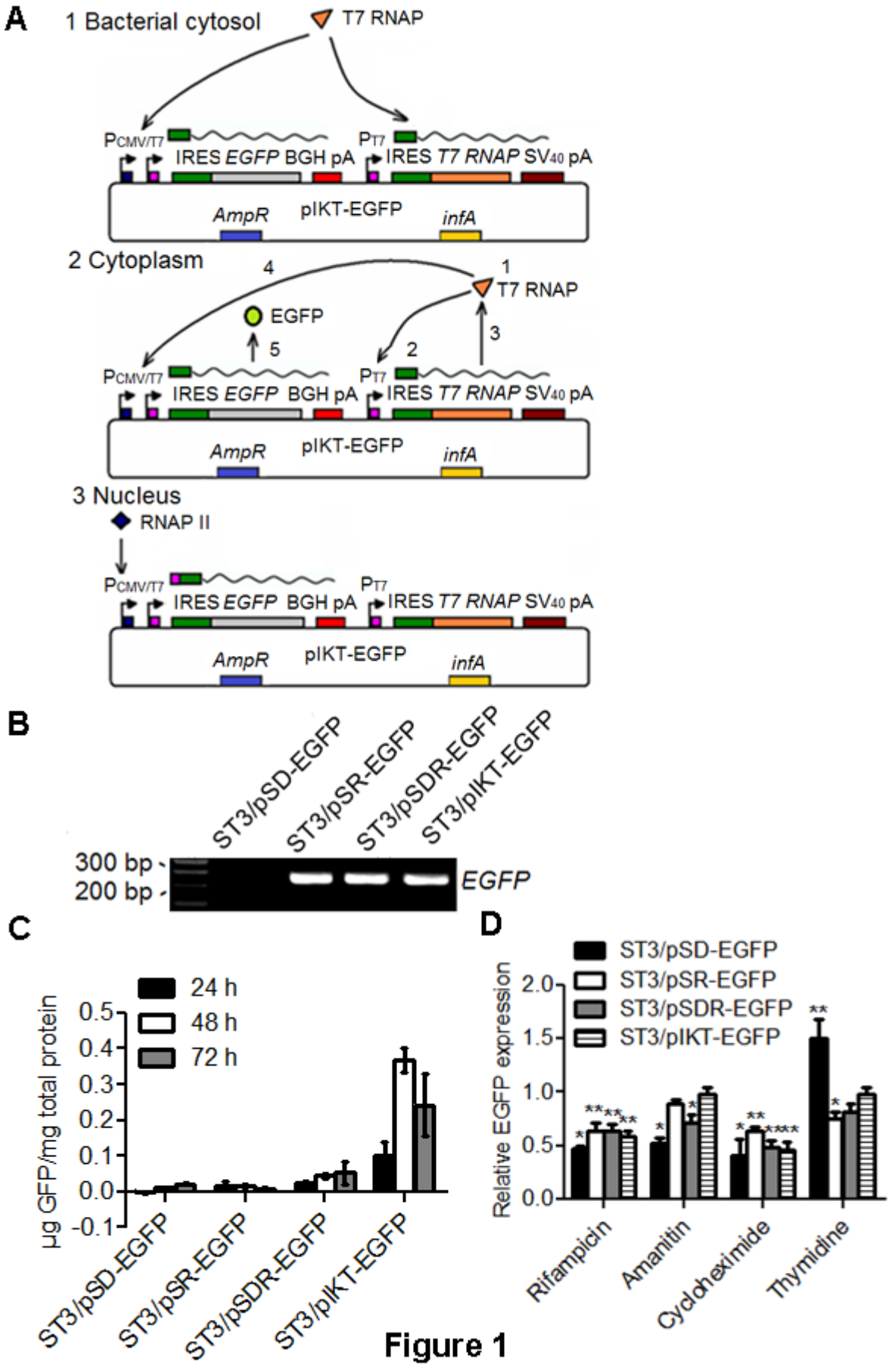
A
1 Bacterial cytosol
T7 RNAP
PCMV/T7
IRES EGFP BGH pA
PT7
IRES T7 RNAP SV40 pA
AmpR
pIKT-EGFP
infA
2 Cytoplasm
4
1
T7 RNAP
EGFP
5
2
3
3 Nucleus
RNAP II
B
ST3/pSD-EGFP
ST3/pSR-EGFP
ST3/pSDR-EGFP
ST3/pIKT-EGFP
300 bp
200 bp
EGFP
C
μg GFP/mg total protein
24 h
48 h
72 h
D
Relative EGFP expression
Rifampicin
Amanitin
Cycloheximide
Thymidine

Figure 1

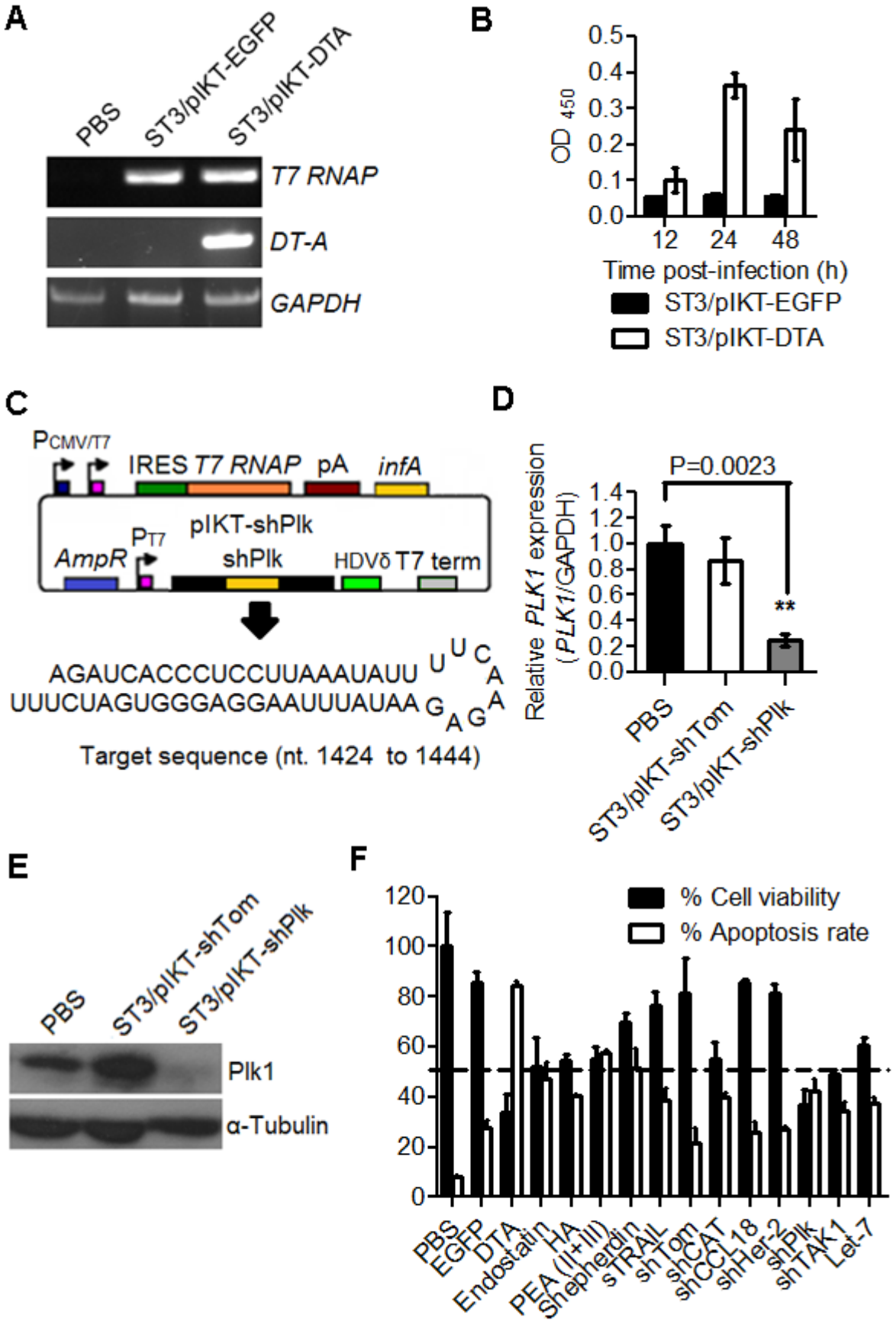
A
PBS
ST3/pIKT-EGFP
ST3/pIKT-DTA
T7 RNAP
DT-A
GAPDH
B
OD 450
0.5
0.4
0.3
0.2
0.1
0.0
12
24
48
Time post-infection (h)
ST3/pIKT-EGFP
ST3/pIKT-DTA
C
PCMV/T7
IRES T7 RNAP
pA
infA
pIKT-shPlk
PT7
AmpR
shPlk
HDVδ T7 term
AGAUCACCCUCCUUAAAUAUU
UUUCUAGUGGGAGGAAUUUAUAA
Target sequence (nt. 1424 to 1444)
D
Relative PLK1 expression
(PLK1/GAPDH)
P=0.0023
**
1.4
1.2
1.0
0.8
0.6
0.4
0.2
0.0
PBS
ST3/pIKT-shTom
ST3/pIKT-shPlk
E
PBS
ST3/pIKT-shTom
ST3/pIKT-shPlk
Plk1
α-Tubulin
F
% Cell viability
% Apoptosis rate
120
100
80
60
40
20
0
PBS
EGFP
DTA
Endostatin
HA
PEA (II+III)
Shepherdin
sTRAIL
shTom
shCAT
shCCL18
shHer-2
shPlk
shTAK1
Let-7

Figure 2

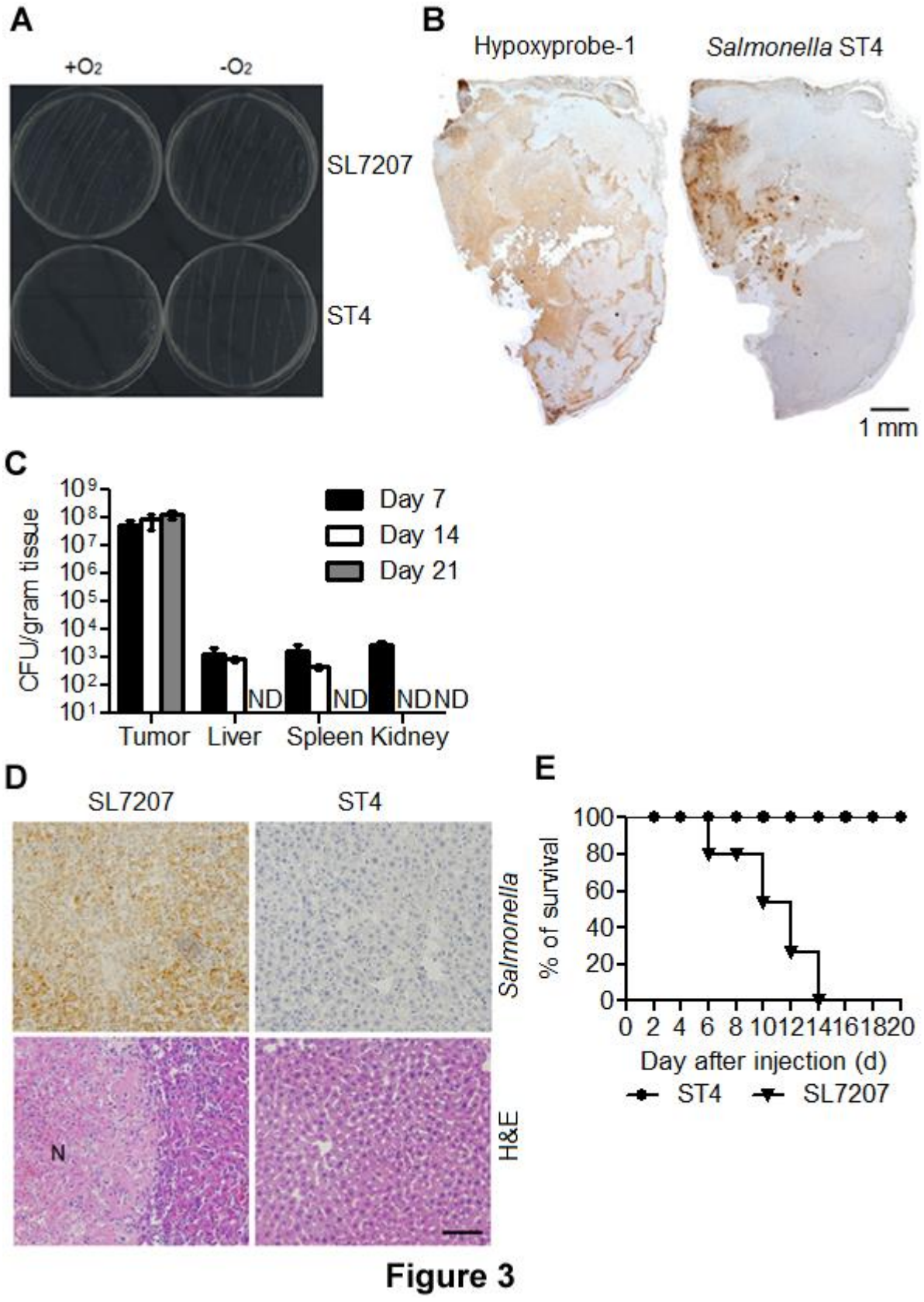
A
+O2
-O2
SL7207
ST4
B
Hypoxyprobe-1
Salmonella ST4
1 mm
C
CFU/gram tissue
Day 7
Day 14
Day 21
ND
ND
ND
ND
Tumor
Liver
Spleen
Kidney
D
SL7207
ST4
Salmonella
H&E
N
E
% of survival
Day after injection (d)
ST4
SL7207

Figure 3

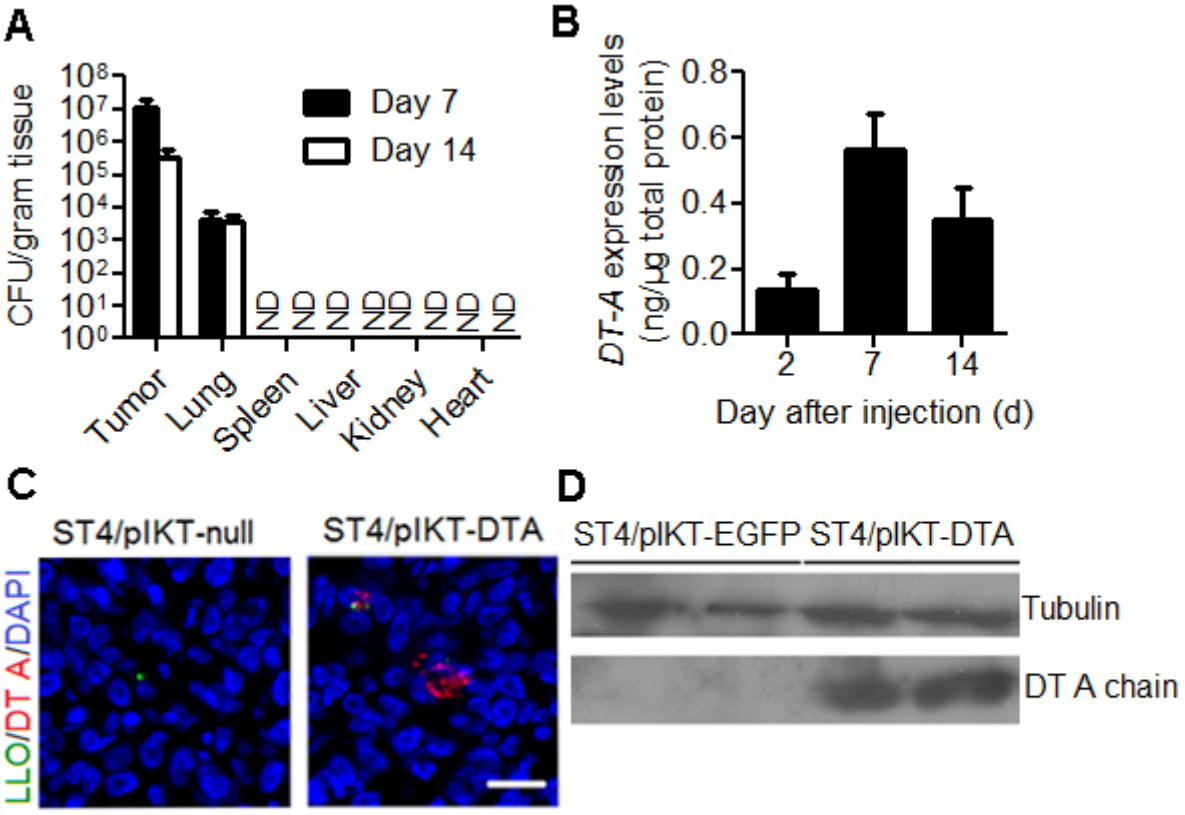
A
CFU/gram tissue
Day 7
Day 14
ND
Tumor
Lung
Spleen
Liver
Kidney
Heart
B
DT-A expression levels
(ng/μg total protein)
Day after injection (d)
C
ST4/pIKT-null
ST4/pIKT-DTA
LLO/DT A/DAPI
D
ST4/pIKT-EGFP
ST4/pIKT-DTA
Tubulin
DT A chain

Figure 4

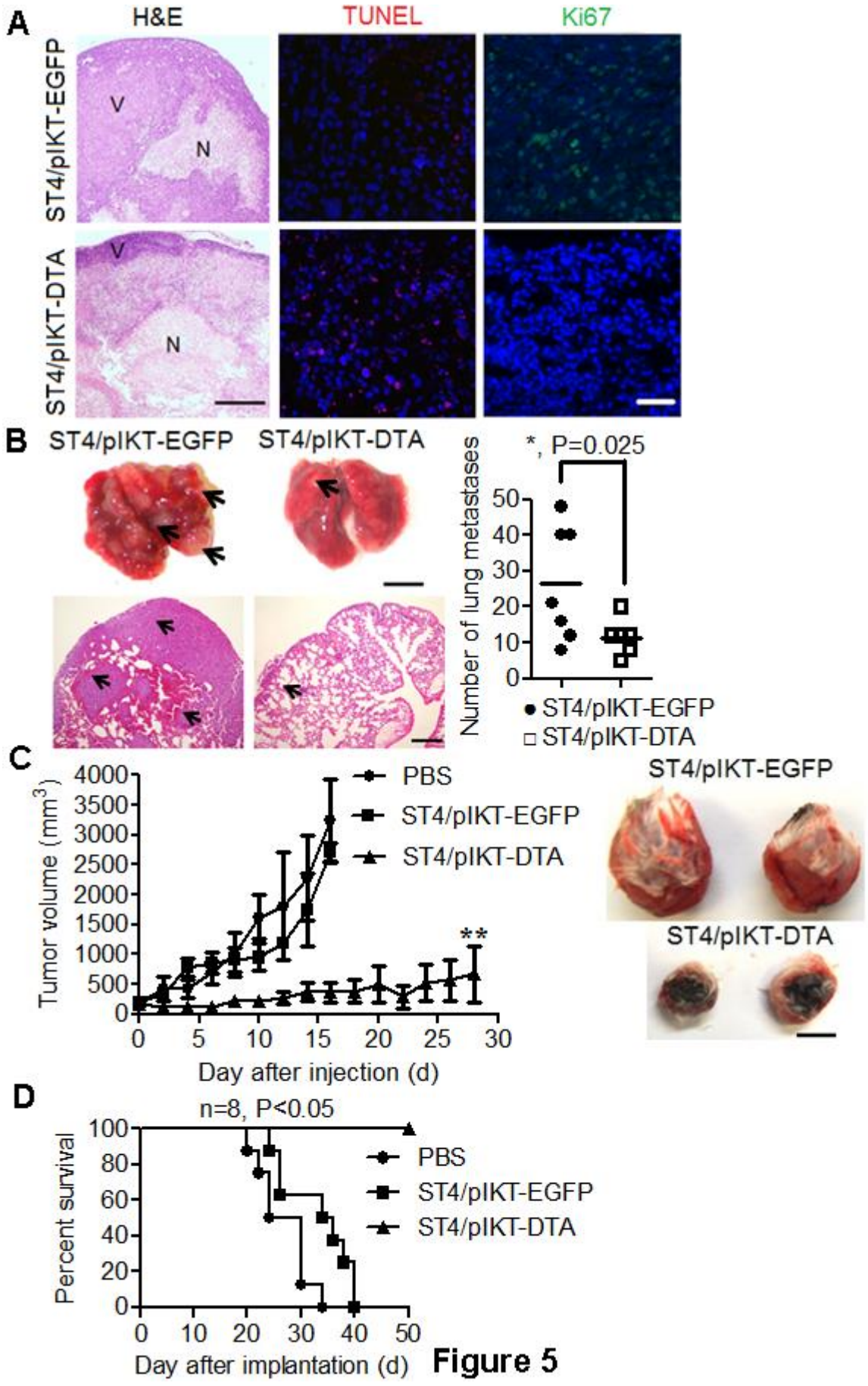
A
H&E
TUNEL
Ki67
ST4/pIKT-EGFP
ST4/pIKT-DTA
V
N
B
ST4/pIKT-EGFP
ST4/pIKT-DTA
*, P=0.025
Number of lung metastases
50
40
30
20
10
0
ST4/pIKT-EGFP
ST4/pIKT-DTA
C
Tumor volume (mm3)
4000
3500
3000
2500
2000
1500
1000
500
0
PBS
ST4/pIKT-EGFP
ST4/pIKT-DTA
**
0
5
10
15
20
25
30
Day after injection (d)
ST4/pIKT-EGFP
ST4/pIKT-DTA
D
n=8, P<0.05
Percent survival
100
80
60
40
20
0
PBS
ST4/pIKT-EGFP
ST4/pIKT-DTA
0
10
20
30
40
50
Day after implantation (d)

Figure 5

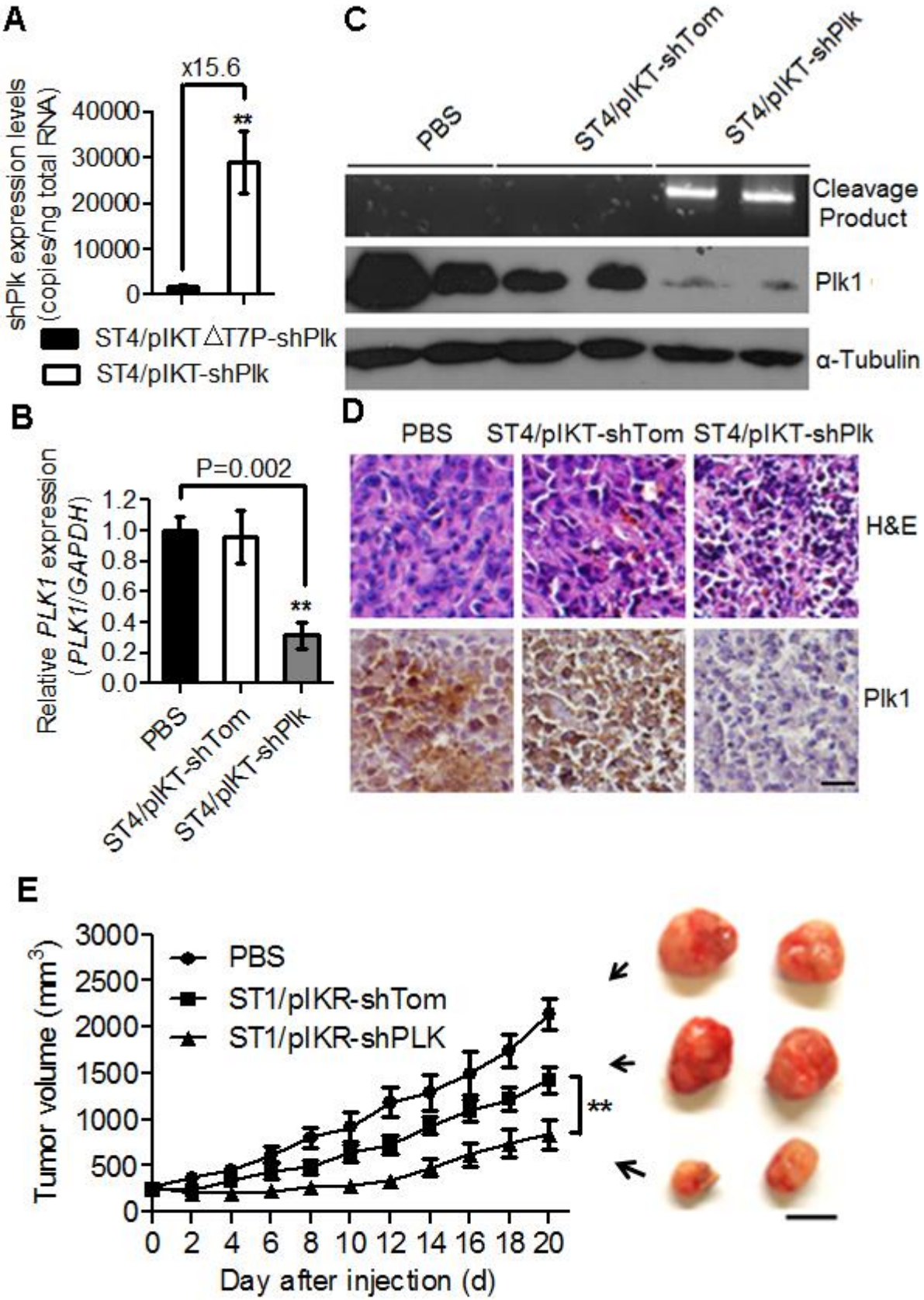
A
x15.6
**
shPlk expression levels (copies/ng total RNA)
40000
30000
20000
10000
0
ST4/pIKTΔT7P-shPlk
ST4/pIKT-shPlk
B
P=0.002
**
Relative PLK1 expression (PLK1/GAPDH)
1.2
1.0
0.8
0.6
0.4
0.2
0.0
PBS
ST4/pIKT-shTom
ST4/pIKT-shPlk
C
PBS
ST4/pIKT-shTom
ST4/pIKT-shPlk
Cleavage Product
Plk1
α-Tubulin
D
PBS
ST4/pIKT-shTom
ST4/pIKT-shPlk
H&E
Plk1
E
Tumor volume (mm3)
3000
2500
2000
1500
1000
500
0
PBS
ST1/pIKR-shTom
ST1/pIKR-shPLK
**
0 2 4 6 8 10 12 14 16 18 20
Day after injection (d)

Figure 6

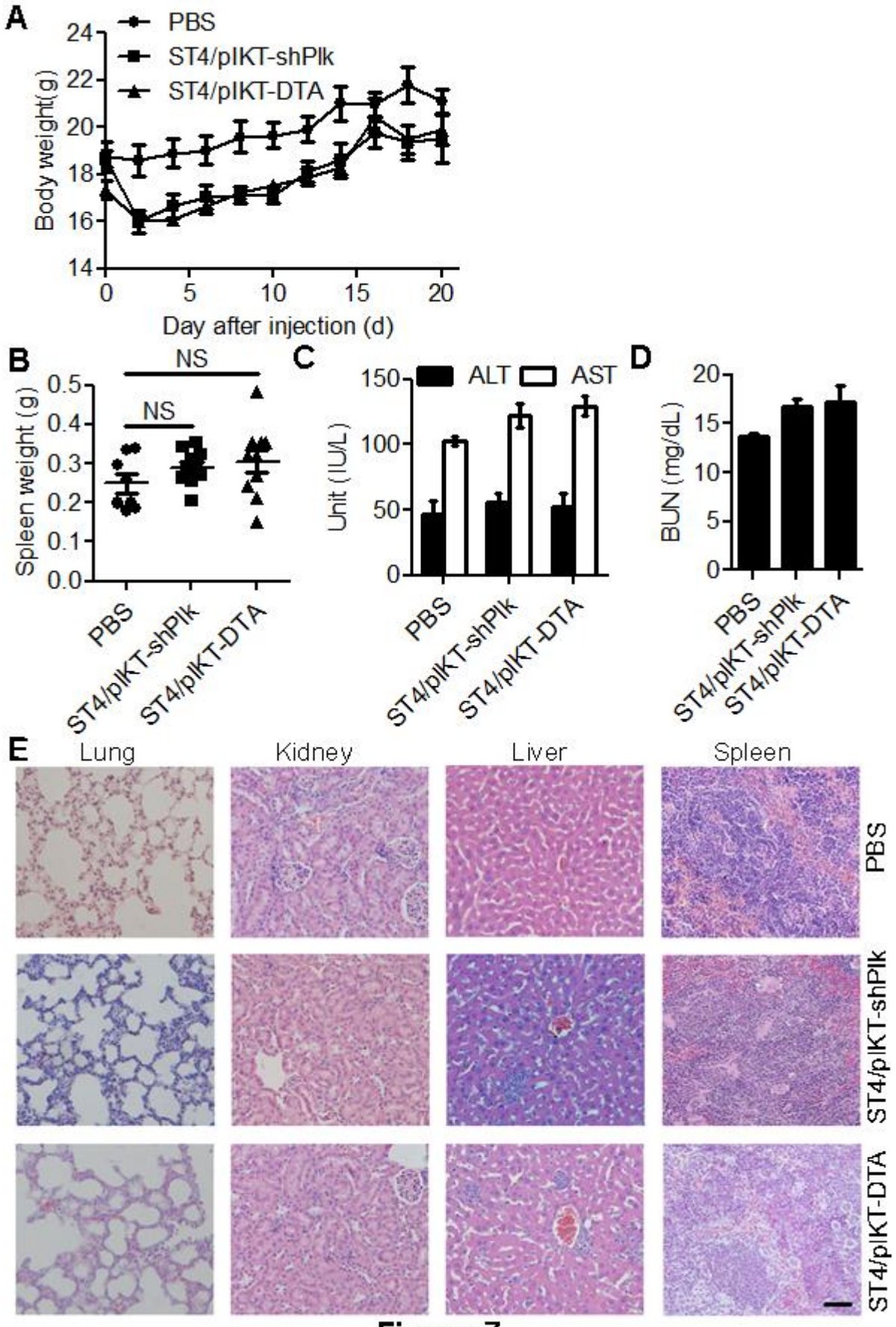
A
PBS
ST4/pIKT-shPlk
ST4/pIKT-DTA
Body weight(g)
Day after injection (d)
B
NS
NS
Spleen weight (g)
PBS
ST4/pIKT-shPlk
ST4/pIKT-DTA
C
ALT
AST
Unit (IU/L)
D
BUN (mg/dL)
E
Lung
Kidney
Liver
Spleen
PBS
ST4/pIKT-shPlk
ST4/pIKT-DTA

Figure 7

Supplementary materials

Table S1. Bacterial strains and plasmids used in this study.

Table S2. Oligonuclotides used in this study.

Table S3. Potential candidates tested *in vitro*.

Table S4. Estimate plasmid pcDNA3.1-infA copy numbers by relative qualification.

Fig. S1. Generation of a tumor-targeting *Salmonella* strain ST4 for delivery and expression of multiple therapeutic factors.

Fig. S2. Relative fluorescence intensity in the cells infected by ST3 or ST5 carrying commercial plasmid pDsred.

Fig. S3. Fluorescence-activated cell sorting was used to demonstrate EGFP expression after 48 h following bacterial infections.

Fig. S4. Composite images of a whole tumour infected with ST4/pIKT-DTA stained to visualize bacteria (left) and cytotoxic DT A chain (right).

Fig. S5. Injection of ST4/pIKT-DTA significantly retards tumor angiogenesis.

Fig. S6. Potent regression of large established tumors in mice treated with ST4/pIKT-DTA.

Fig. S7. Comparison of anti-tumor effects between *tk*RNAi system (E/TRIP-shRNA) and our system (S/pIKT-shRNA).